



**HAL**  
open science

# Precipitation and temperature anomalies over Aotearoa New Zealand analysed by weather types and descriptors of atmospheric centres of action

Benjamin Pohl, Andrew Sturman, James Renwick, Hervé Quénol, Nicolas Fauchereau, Andrew Lorrey, Julien Pergaud

## ► To cite this version:

Benjamin Pohl, Andrew Sturman, James Renwick, Hervé Quénol, Nicolas Fauchereau, et al.. Precipitation and temperature anomalies over Aotearoa New Zealand analysed by weather types and descriptors of atmospheric centres of action. *International Journal of Climatology*, 2023, 43, pp.331-353. 10.1002/joc.7762 . hal-03720488

**HAL Id: hal-03720488**

**<https://hal.science/hal-03720488>**

Submitted on 12 Jul 2022

**HAL** is a multi-disciplinary open access archive for the deposit and dissemination of scientific research documents, whether they are published or not. The documents may come from teaching and research institutions in France or abroad, or from public or private research centers.


L'archive ouverte pluridisciplinaire **HAL**, est destinée au dépôt et à la diffusion de documents scientifiques de niveau recherche, publiés ou non, émanant des établissements d'enseignement et de recherche français ou étrangers, des laboratoires publics ou privés.



Distributed under a Creative Commons Attribution - NoDerivatives 4.0 International License

## RESEARCH ARTICLE

# Precipitation and temperature anomalies over Aotearoa New Zealand analysed by weather types and descriptors of atmospheric centres of action

Benjamin Pohl<sup>1</sup>  | Andrew Sturman<sup>2</sup> | James Renwick<sup>3</sup> | Hervé Quénol<sup>4</sup> |  
Nicolas Fauchereau<sup>5</sup> | Andrew Lorrey<sup>5</sup> | Julien Pergaud<sup>1</sup>

<sup>1</sup>UMR6282 Biogéosciences, CNRS, Université de Bourgogne Franche-Comté, Dijon, France

<sup>2</sup>School of Earth and Environment, University of Canterbury, Christchurch, New Zealand

<sup>3</sup>School of Geography, Environment & Earth Sciences, Victoria University of Wellington, Wellington, New Zealand

<sup>4</sup>UMR6554 LETG CNRS, Université Rennes 2, Rennes, France

<sup>5</sup>National Institute of Water and Atmospheric Research, Auckland, New Zealand

## Correspondence

Benjamin Pohl, Laboratoire Biogéosciences, 6 bvd. Gabriel, 21000 Dijon, France.  
Email: [benjamin.pohl@u-bourgogne.fr](mailto:benjamin.pohl@u-bourgogne.fr)

## Abstract

Weather types (WTs) are often used to assess the relationships between synoptic-scale atmospheric dynamics and local scale climate anomalies. We focus here on Aotearoa New Zealand (ANZ) where pre-existing WT types have recently been characterized using a set of descriptors monitoring the daily location and intensity of their main atmospheric centres of action (ACAs). We show here that the precipitation and temperature anomalies associated with the WT types in ANZ are more complex than previously thought. They do not solely depend on type occurrence, but are also strongly modulated by within-type changes in the location and intensity of ACAs, and their interaction with surface terrain. Thus, the mere analysis of WT occurrence is not sufficient to explain climate variability over ANZ. The magnitude and sign of daily minimum and maximum temperature anomalies are strongly driven by meridional advection of temperature, which is also driven by within-type changes in ACAs. The amplitude of precipitation anomalies is likewise strongly variable within WT types. Associated mechanisms involve interactions between the underlying terrain and atmospheric fluxes modulated by ACAs, modifying the strength and location of orographic uplift. Finally, daily extreme precipitation can occur under several cyclonic WT types, more particularly when their low-pressure ACAs are significantly more intense than normal. This situation is associated with more intense moisture transport towards ANZ, promoting heavy precipitation there. These results provide a detailed assessment of within-type variability in temperature and precipitation patterns at both synoptic and local scales. They also help to improve understanding of local effects of larger scale synoptic patterns, thereby allowing for more accurate use of analogues in forecasting.

## KEYWORDS

Aotearoa New Zealand, atmospheric centres of action, precipitation, southern mid-latitudes, synoptic variability, temperature, weather types

This is an open access article under the terms of the [Creative Commons Attribution-NonCommercial-NoDerivs](https://creativecommons.org/licenses/by-nc-nd/4.0/) License, which permits use and distribution in any medium, provided the original work is properly cited, the use is non-commercial and no modifications or adaptations are made.

© 2022 The Authors. *International Journal of Climatology* published by John Wiley & Sons Ltd on behalf of Royal Meteorological Society.

## 1 | INTRODUCTION

Weather types (WTs hereafter: e.g., Michelangeli *et al.*, 1995; Cassou *et al.*, 2004; Straus *et al.*, 2007; Eden *et al.*, 2014) are commonly used in climate science to concisely characterize and understand regional circulation and variability. The approach consists of identifying a limited number of recurrent WT (and/or groups of WT into atmospheric regimes) and then using their timing and/or frequency changes to investigate processes driving regional climate patterns at daily to multidecadal scales (Lorrey *et al.*, 2007; Fauchereau *et al.*, 2009; Parsons *et al.*, 2014; Moron *et al.*, 2018; Pohl *et al.*, 2018; Champagne *et al.*, 2019). However, WT commonly oversimplify the spatiotemporal variability of climate, which is continuous by nature, by discretizing it into a small number of configurations that poorly or only partly reflect the complexity of daily weather and climate. As a consequence, climate phenomena and processes that are associated with moderate variance tend to be less efficiently described by WT. This is especially the case for low-frequency climate variability, so that long-term changes in the state of the climate system tend to occur within the types, rather than appearing as changes in type occurrence (Pohl and Fauchereau, 2012; Pohl *et al.*, 2018; Champagne *et al.*, 2019). Although many papers recognize within-type changes as significant, very few have analysed them in detail.

In order to address these limitations, and improve the WT methodology, a recent paper (Pohl *et al.*, 2021b; P21 hereafter) introduced a set of quantitative descriptors to monitor the location (latitude, longitude) and intensity (amplitude of daily minimum or maximum geopotential height anomalies at regional scale) of atmospheric centres of action (ACA hereafter: either atmospheric highs or lows). These descriptors are qualitatively different from one WT to another, depending on the presence of any perturbation associated with the type composite mean field. They allow for a detailed quantification of the strength of the atmospheric systems and refine the analysis of weather and climate variability occurring within each WT. P21 based their work on the 12 types developed by Kidson (2000, K2K hereafter) over the Aotearoa New Zealand (ANZ) sector. These types monitor synoptic-scale atmospheric highs or lows that develop in the mid-latitude westerlies and act to disturb them in return. Focusing on large-scale mechanisms, P21 identified significant teleconnections between the WT descriptors and the Southern Annular Mode (SAM) in the southern high latitudes, and El Niño–Southern Oscillation (ENSO) in the tropical Pacific. These modes of large-scale variability, known to modulate the regional climate in the ANZ sector (Jiang *et al.*, 2004; 2013b; Renwick and

Thompson, 2006; Ummenhofer and England, 2007; Kidston *et al.*, 2009; Ummenhofer *et al.*, 2009; Jiang, 2011) were found to have a larger influence on ACA descriptors, that is, the WT's intrinsic properties, than their frequencies.

P21 also concluded that studies at finer spatial scales are needed in order to assess how regional-scale atmospheric dynamics (as inferred both by WT and variability in their associated ACA) interact with the complex topography of ANZ (Figure 1) to modulate regional climate patterns. Interactions between topography, land–sea contrast and regional atmospheric dynamics have been investigated in many previous studies, from a local to regional climate point of view (e.g., Salinger, 1979; 1980a; 1980b; McCauley and Sturman, 1999; Sturman *et al.*, 1999; Sturman and Wanner, 2001). The marked and complex relief of ANZ has a very strong effect (e.g., Renwick, 2011) on modulating the spatial patterns of temperature (through vertical and horizontal gradients) and precipitation (through contrasted exposures and upwind/downwind effects under the dominant mid-latitude westerly winds). Together with the Andes in South America, ANZ a major topographic barrier at these latitudes of the Southern Hemisphere. While these barriers are likely to perturb atmospheric fluxes, they are also under the influence of the strong westerly wind belt and the transient perturbations, embedded in the mid-latitude dynamics (Pepler *et al.*, 2018; 2019), and represented here by the 12 types of K2K.

How these WT modulate precipitation and temperature anomalies over ANZ has already been discussed in previous studies (K2K; Ackerley *et al.*, 2011; Jiang, 2011; Renwick, 2011; Jiang *et al.*, 2013a; Fauchereau *et al.*, 2016; Gibson *et al.*, 2016). However, air temperature anomalies associated with the WT have been only partly analysed to date, and corresponding physical mechanisms have not been established. Similarly, although relationships between regional WT and precipitation anomalies in ANZ have previously been addressed (K2K; Jiang *et al.*, 2004; 2013b; Renwick, 2011; Gibson *et al.*, 2016), these studies have focused on changes in daily precipitation amounts, with limited assessment of mechanisms. Moreover, whether these WT yield quasi-stationary climate anomalies, or whether the latter are modified by WT's internal characteristics, is an issue that remains to be explored. Finally, how these WT and their corresponding main ACA relate to daily extremes of precipitation and air temperature across ANZ remains unclear to date. The present paper aims to address these questions.

Hence, this work aims at establishing the relationships between surface climate variables in ANZ (namely, daily minimum and maximum air temperature and daily

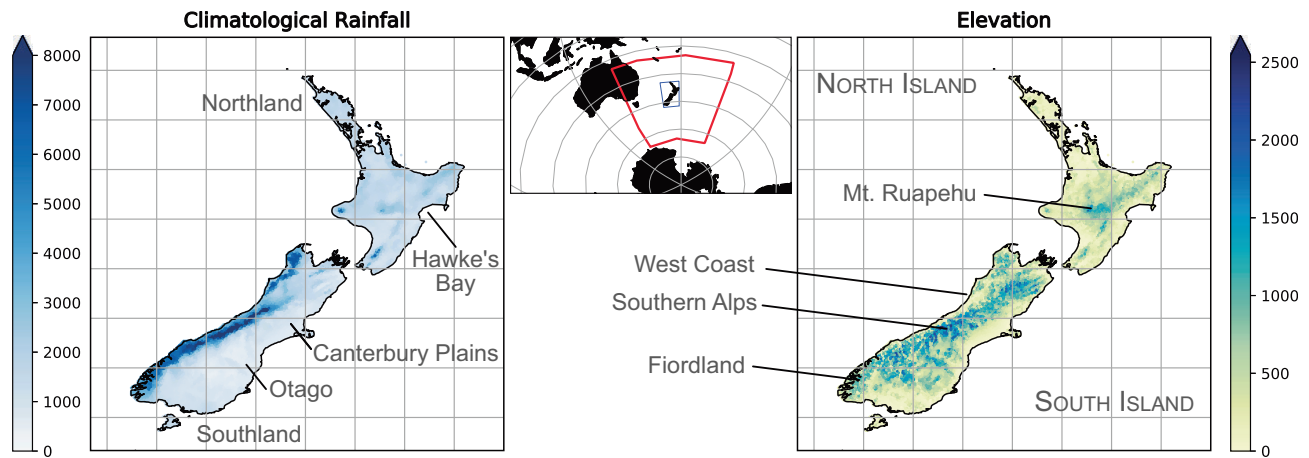


**FIGURE 1** Map of Aotearoa New Zealand (ANZ). Left panel: climatological mean annual precipitation amounts (mm: left colour bar) according to VCSN data, period 1979–2019. Right panel: elevation (m above sea level: right colour bar). Central panel shows the location of ANZ and the domain boundaries used for weather regime analysis (in red) and regional climate anomalies in ANZ (in blue). The names of the regions mentioned in the text are labelled in grey [Colour figure can be viewed at [wileyonlinelibrary.com](http://wileyonlinelibrary.com)]

precipitation amounts) and the diversity of synoptic configurations, considering both inter-type and within-type variations. The latter is estimated by changes in the strength and location of the main ACAs associated with the WTs. Finally, we focus on daily (temperature and rainfall) extremes, in order to assess the extent to which WTs conducive to climate extremes differ synoptically from their other occurrences.

Section 2 presents the datasets used, the WT classification and the descriptors associated with their main ACAs. Section 3 focuses on temperature anomalies, as modulated by these WTs and their descriptors, and addresses associated regional-scale mechanisms. Section 4 extends these results to precipitation anomalies. Section 5 considers the case of daily extremes (of precipitation and temperature). Section 6 summarizes the main results and provides concluding remarks.

## 2 | DATA AND METHODS

### 2.1 | Data

Atmospheric fields used in this study are taken from the ERA5 ensemble reanalysis (Hersbach *et al.*, 2020). ERA5 is the fifth generation of the atmospheric reanalysis released by the European Centre for Medium-Range Weather Forecasts. It currently covers the period 1979 onwards (with an experimental extension to 1950) and includes a 10-member ensemble to quantify uncertainties associated with the density and quality of the assimilated data (see also P21). In this work, we use the regular  $0.5^\circ \times 0.5^\circ$  grids of the ensemble over the period 1979–

2019 for the following atmospheric variables: daily mean fields of geopotential height at 1,000 (Z1000, m) and 700 hPa (Z700, m), 2 m air temperature ( $^\circ\text{C}$ ) and specific humidity (converted to  $\text{g}\cdot\text{kg}^{-1}$ ), surface solar radiation (converted to  $\text{W}\cdot\text{m}^{-2}$ ), total water in the air column ( $\text{kg}\cdot\text{m}^{-2}$ ), vertical velocity of the wind at 850 hPa ( $\text{Pa}\cdot\text{s}^{-1}$ ), and finally, the zonal ( $u$ ) and meridional ( $v$ ) components of the horizontal wind ( $\text{m}\cdot\text{s}^{-1}$ ) at 10 m and 700 hPa.

Daily rainfall and temperature data for ANZ come from the National Institute of Water and Atmospheric Research (NIWA) Virtual Climate Station Network (VCSN). Data coverage for the NIWA VCSN (Tait and Turner, 2005; Tait *et al.*, 2006; 2012) is available from 1972 to the present for 13 daily climate variables on a  $5 \times 5$  km grid covering the country. The approach to generating the NIWA VCSN uses a thin-plate smoothing spline model for spatial interpolation between in situ station data, incorporating two location variables (latitude and longitude) and a third “pattern” variable. For daily minimum ( $T_n$ ) and maximum ( $T_x$ ) temperature, elevation (Figure 1) was included in the model. For precipitation, a digital version of an expert-guided 1951–1980 mean annual rainfall isohyet map was used as the pattern variable as a way to represent orographic influences that arise from prevailing circulation interacting with mountainous terrain. VCSN data provide biased estimates of precipitation, especially in the most elevated parts of the country where the density of rain-gauges and weather stations is much reduced (Tait *et al.*, 2012; Mason *et al.*, 2017). VCSN estimated temperature generally shows weaker biases (Mason *et al.*, 2017).

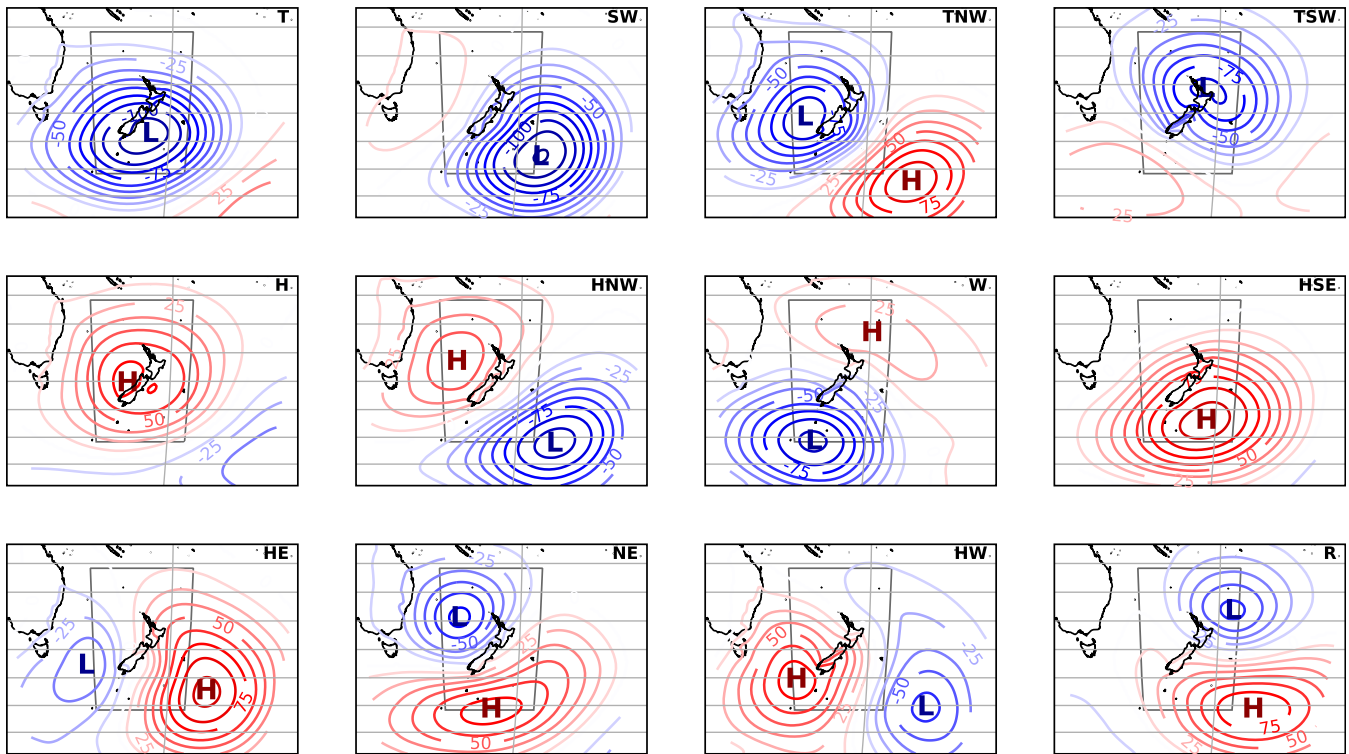


**FIGURE 2** Z1000 anomalies (m: contours) associated with the 12 KT's over the period 1979–2019. Anomalies that are not statistically significant at the 95% level are shaded white. The inner rectangle represents the domain used by Kidson (2000). H: local maximum Z1000 anomalies. L: local minimum Z1000 anomalies [Colour figure can be viewed at [wileyonlinelibrary.com](http://wileyonlinelibrary.com)]

## 2.2 | Weather type redefinition using the ERA5 ensemble

As in P21, this study uses the WT classification of K2K over the ANZ sector. The corresponding 12 WTs, originally based on 12-hourly maps of Z1000 derived from NCEP/NCAR reanalyses, are updated here using ERA5 daily ensemble fields. Two WT time distributions are therefore considered, the original WT classification based on NCEP/NCAR timing, and the redefined distribution obtained by ascribing each day of each member based on ERA5, over the period 1979–2019, to its nearest type centroid. These two type definitions are seen to differ, with roughly 35% of the days of the period not being ascribed to the same WT. However, the composite mean fields are very similar, because day swaps between types are associated with similar patterns that differ only in the location of ACAs. The latter are expected to be more precisely defined by ERA5 data due to its much higher spatial resolution. All results and conclusions discussed below can be obtained with both WT distributions. More details and a comparison between both WT timings are given in P21.

In addition to the partitioning into 12 discrete WTs, we reuse here the descriptors from P21 that monitor the location and intensity of the main ACAs associated with each type. These descriptors are derived from Z1000 daily

anomalies (noted Z1000'), after removing the mean annual cycle (Figure 2). This approach differs from K2K and subsequent studies (e.g., Ackerley *et al.*, 2011; Renwick, 2011; Fauchereau *et al.*, 2016; Gibson *et al.*, 2016; Cullen *et al.*, 2019, among many others), who only considered raw Z1000 fields. Three groups of WTs are formed, depending on the presence or absence of regional extremes of Z1000' (Figure 2 and Table 1). The “Low” group has only one such extreme, consisting of a regional minimum of Z1000' denoting an atmospheric trough. Conversely, the “High” group only includes a regional maximum of Z1000', indicative of an atmospheric ridge. The “Gradient” group has both extremes. The descriptors defined in P21 qualitatively differ from one group of WTs to another. For the “Low” group, three metrics depict the intensity of the low, corresponding to the minimum Z1000' value within the whole domain ( $\text{Min}_{Z'}$ ), and its corresponding latitude and longitude (Lat, Lon) defining the location of the low ACA. The “High” types use the same metrics, but applied to the Z1000' maximum to define the high ACA. The “Gradient” types use both metrics (Table 1), with additional ones used to depict the relative position and differences between both ACAs. This provides the difference between Z1000' maximum and minimum ( $\text{Diff}_{Z'}$ ), the latitudinal and longitudinal differences in their locations ( $\text{Diff}_{\text{Lat}}$ ,  $\text{Diff}_{\text{Lon}}$ ), and finally the slope of the geopotential

**TABLE 1** Overview of the internal descriptors used for each of the 12 KT (in rows, with their usual abbreviations and their long names after Ackerley *et al.*, 2011 and Cullen *et al.*, 2019)

	Low (trough)			High (ridge)			Gradient (trough and ridge)			
	Lat	Lon	Min <sub>z'</sub>	Lat	Lon	Max <sub>z'</sub>	Diff <sub>Lat</sub>	Diff <sub>Lon</sub>	Diff <sub>z'</sub>	Grad
T (trough)	x	x	x							
SW (southwesterly)	x	x	x							
TNW (trough northwesterly)	x	x	x	x	x	x	x	x	x	x
TSW (trough southwesterly)	x	x	x							
H (high)				x	x	x				
HNW (high to the northwest)	x	x	x	x	x	x	x	x	x	x
W (westerly)	x	x	x	x	x	x	x	x	x	x
HSE (high to the southeast)				x	x	x				
HE (high to the east)	x	x	x	x	x	x	x	x	x	x
NE (northeasterly)	x	x	x	x	x	x	x	x	x	x
HW (high to the west)	x	x	x	x	x	x	x	x	x	x
R (ridge)	x	x	x	x	x	x	x	x	x	x

Note: “Low” columns are for troughs, “High” columns for ridges, and “Gradient” columns for weather types showing both troughs and ridges. Internal descriptors depict the spatial coordinates (Lat, Lon) and intensities (Min<sub>z'</sub>, Max<sub>z'</sub>) of centres of action, and for gradient types, their differences (Diff<sub>Lat</sub>, Diff<sub>Lon</sub>, Diff<sub>z'</sub>). Grad corresponds to the geopotential height gradient between both centres of action (see text for further details).

height gradient, defined as  $\text{Grad} = \text{Diff}_{z'} / \sqrt{\text{Diff}_{\text{Lat}}^2 + \text{Diff}_{\text{Lon}}^2}$ . In the following, the within-type variability is studied by considering the opposite polarities of all these descriptors. To that end, we use their 20th and 80th percentiles, noting that some of the days present in these samples overlap those used to extract the opposite polarities of other descriptors (P21). In good approximation, the descriptors monitoring the zonal and meridional locations of the ACAs are only weakly related (i.e., are statistically independent) for WTs associated with one single ACA (either Low or High). For the Gradient-type WTs, all differential indices between the opposite ACAs are, logically, partly determined by the location and intensity of each ACA (P21).

Here, we analyse how these descriptors relate to fine-scale temperature and precipitation anomalies across ANZ, while focus was given in P21 on the relationship between the ACA descriptors and large-scale climate variability. All descriptors are quantitative and thus help address one of the main weaknesses of the WT approach, which is in discretizing naturally continuous climate variability (P21). The effect of descriptors on regional climate is assessed through composite analyses based on the opposite polarities of each descriptor. Differences are tested using Welch's *t* tests (an evolution of Student's *t* test that does not assume the variance of the two considered samples to be equal). Although all types are important to drive the local to regional climate, in the following we consider more closely two types out of the 12 identified by K2K, namely, types HSE and T (please

refer to Table 1 for the long names of the types). These two types are chosen as case studies because (a) they both display strong within-type variability; (b) they both favour climate extremes over large parts of ANZ, for daily precipitation amounts for type T and daily maximum air temperature for type HSE; (c) because of (b), they are both important for climate impacts on regional societies, infrastructure and environment. Other types are discussed in Supporting Information.

### 2.3 | Estimation of orographic lifting

The modulation of daily precipitation amounts in ANZ by the synoptic weather patterns is hypothesized to result from the differing exposure of local terrain to regional-scale atmospheric circulation in the lower troposphere. Following Kyriakidis *et al.* (2001), the associated orographic lifting  $W$  is computed here as the inner product of directional elevation gradients with the interpolated 700-hPa horizontal winds (Equation (1)),

$$W = -\mathbf{V} \cdot \nabla h = - \left[ u \left( \frac{\partial h}{\partial x} \right) + v \left( \frac{\partial h}{\partial y} \right) \right], \quad (1)$$

where  $\mathbf{V} = (u, v)$  is the horizontal wind vector as depicted by its zonal  $u$  and meridional  $v$  components, and  $\partial h / \partial x$  and  $\partial h / \partial y$  denote the local gradients of elevation along the same (longitudinal and latitudinal) directions. These

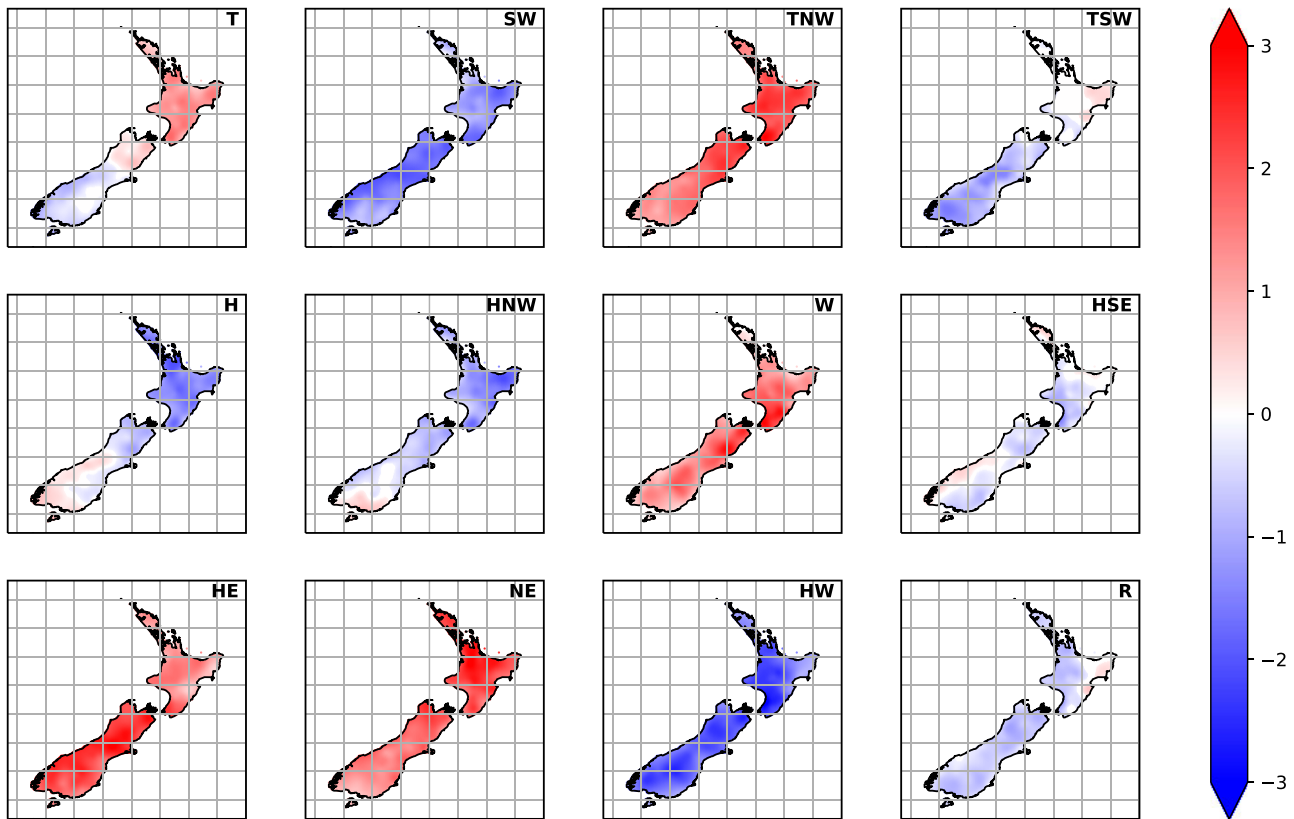


**FIGURE 3** Daily Tn anomalies ( $^{\circ}\text{C}$ : colours) associated with the 12 weather types of Kidson (2000) over the period 1979–2019. Anomalies that are not statistically significant at the 95% level according to a 1-tailed  $t$  test are shaded white [Colour figure can be viewed at [wileyonlinelibrary.com](http://wileyonlinelibrary.com)]

gradients are calculated based on the digital elevation model used in VCSN data (section 2.1) (Figure 1). As in Kyriakidis *et al.* (2001),  $V$  is derived here from 700-hPa zonal and meridional components of the wind. The approach is usually used in statistical downscaling to produce fine-scale estimation of precipitation (Kyriakidis *et al.*, 2001). It is used here to provide an estimation of the strength of the orographic forcing resulting from terrain elevation and lower-tropospheric circulation, the latter being itself often modulated by synoptic-scale ACAs. This approach was also successfully used to separate surface and dynamical forcings under various synoptic contexts in a tropical island with complex terrain (Morel *et al.*, 2014), including analysis of precipitation extremes (Pohl *et al.*, 2016).

### 3 | DAILY MINIMUM AND MAXIMUM AIR TEMPERATURE ANOMALIES

#### 3.1 | Temperature anomaly patterns

K2K proposed a simple categorization of above normal, neutral or below normal temperature associated with WT

occurrences, by regrouping the latter into three regimes comprising atmospheric ridges, troughs or zonal flow (note that these three regimes or groups do not correspond to those used in section 2 and in P21 to define our ACA descriptors). Renwick (2011) used the same three groups and extended air temperature analysis to composite means of Tn and Tx, considering also austral summer and winter seasons separately. “Troughs” are associated with positive Tn and negative Tx anomalies, and therefore with a reduced diurnal temperature range (DTR). The opposite tends to prevail for ridges, even though strong exposure effects are also found on the South Island because of the topographic barrier formed by the Southern Alps mountain range (Renwick, 2011). Here, we build on these existing findings by (a) assessing daily Tn and Tx anomalies associated with each WT, (b) interpreting within-type diversity using the ACA descriptors, and (c) analysing corresponding atmospheric circulation anomalies in the ANZ sector to assess mechanisms and processes driving temperature variability at regional and local scales.

Figures 3 and 4 present Tn and Tx anomalies over ANZ associated with the 12 WTs of K2K, respectively, thereby updating and completing the results of Renwick

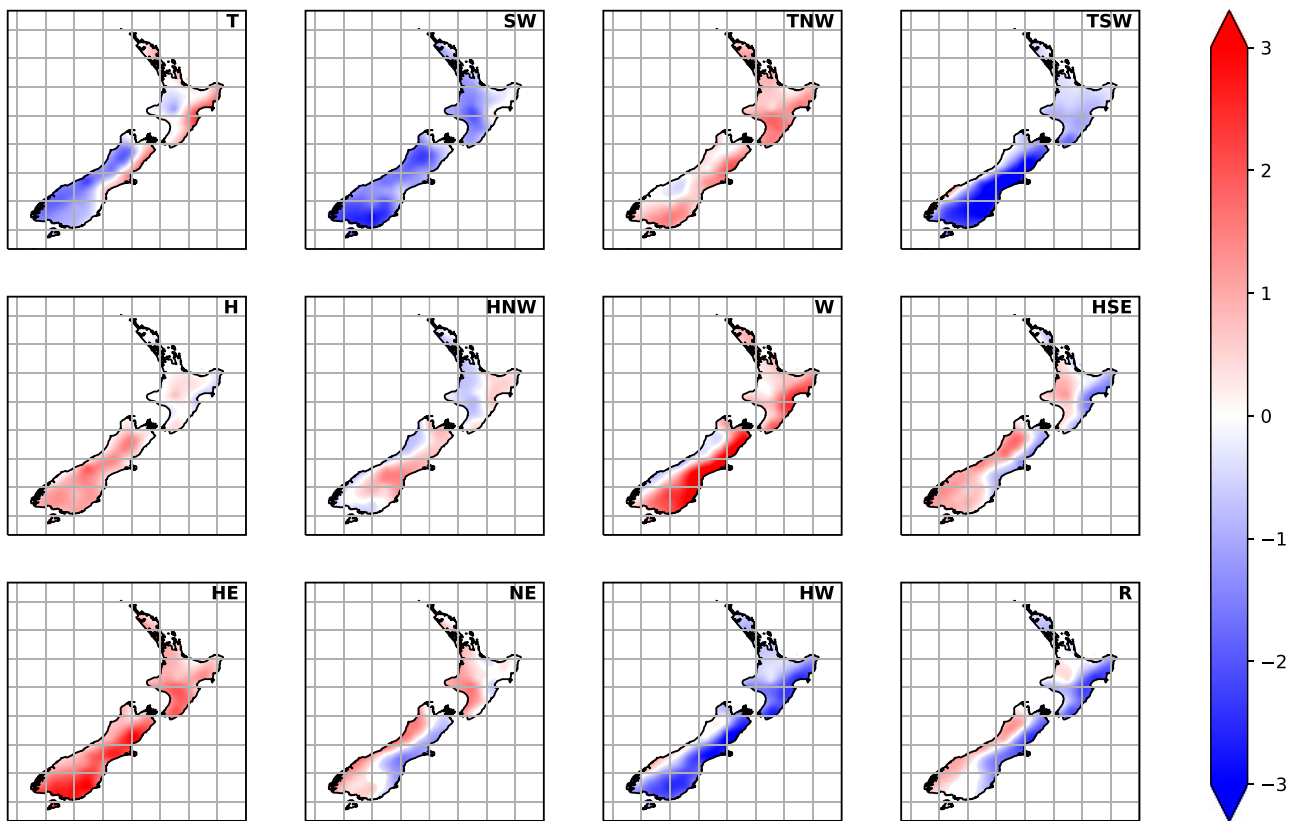


**FIGURE 4** Daily Tx anomalies ( $^{\circ}\text{C}$ : colours) associated with the 12 weather types of Kidson (2000) over the period 1979–2019. Anomalies that are not statistically significant at the 95% level according to a 1-tailed  $t$  test are shaded white [Colour figure can be viewed at [wileyonlinelibrary.com](http://wileyonlinelibrary.com)]

(2011) over the period 1979–2019. All 12 WTs are associated with significant temperature anomalies over most of ANZ, with departures from climatology that often exceed  $\pm 2^{\circ}\text{C}$ . However, some WTs coincide with anomalies of weaker amplitude, on average. This is especially true for Tn (e.g., types HSE and R), with anomalies tending to be spatially coherent, with weak exposure effects. This suggests a weak topographic influence on associated mechanisms, at least at the scale of ANZ. Exposure effects are clearer for Tx, especially in the South Island between the western and eastern slopes of the Southern Alps (Figure 1). Although the general conclusions match those of K2K, it is nonetheless found that members of K2K's “trough” group (regrouping those WTs on the first row: T, SW, TNW, TSW) are each associated with quite contrasting Tn and Tx anomalies. This is even more true for K2K's “blocking” group (types HSE, HE, NE, HW, and R), in which WT differentiation tends to be stronger for Tn than Tx. Renwick (2011) reached similar conclusions over the period 1958–2009. Finally, most types showing strong anomalies in Tn tend to show strong anomalies of the same sign in Tx, albeit with a weaker spatial coherence due to enhanced exposure contrasts. Although DTR is significantly modulated by the WTs

(Renwick, 2011), large-scale mechanisms (such as cold or warm advection) are also at play, which have similar effects on both Tn and Tx and act therefore to cool or warm large parts of the country.

In order to investigate within-type complexity, and its effects on temperature anomalies in ANZ, we consider here the case of type HSE (Figures 5–7). This choice is motivated by (a) the very strong variability in temperature anomalies associated with this type across ANZ and (b) the fact that this type was identified as conducive to near-climatology temperature conditions across ANZ, a result that will be examined further below. HSE is a “blocking” type according to K2K and a “ridge” type according to P21, which means that its Z1000' composite mean pattern includes only one single ACA, corresponding to a regional maximum of Z1000' (Table 1 and Figure 5) located south to southeast of ANZ, hence its name. Thus, three descriptors have been defined for this type, to monitor the location (Lat, Lon) and intensity of the ridge (as inferred by the positive Z1000' extreme in the domain, for each day of each member ascribed to this type). The statistical distribution and seasonal dependency of these descriptors are given in P21.



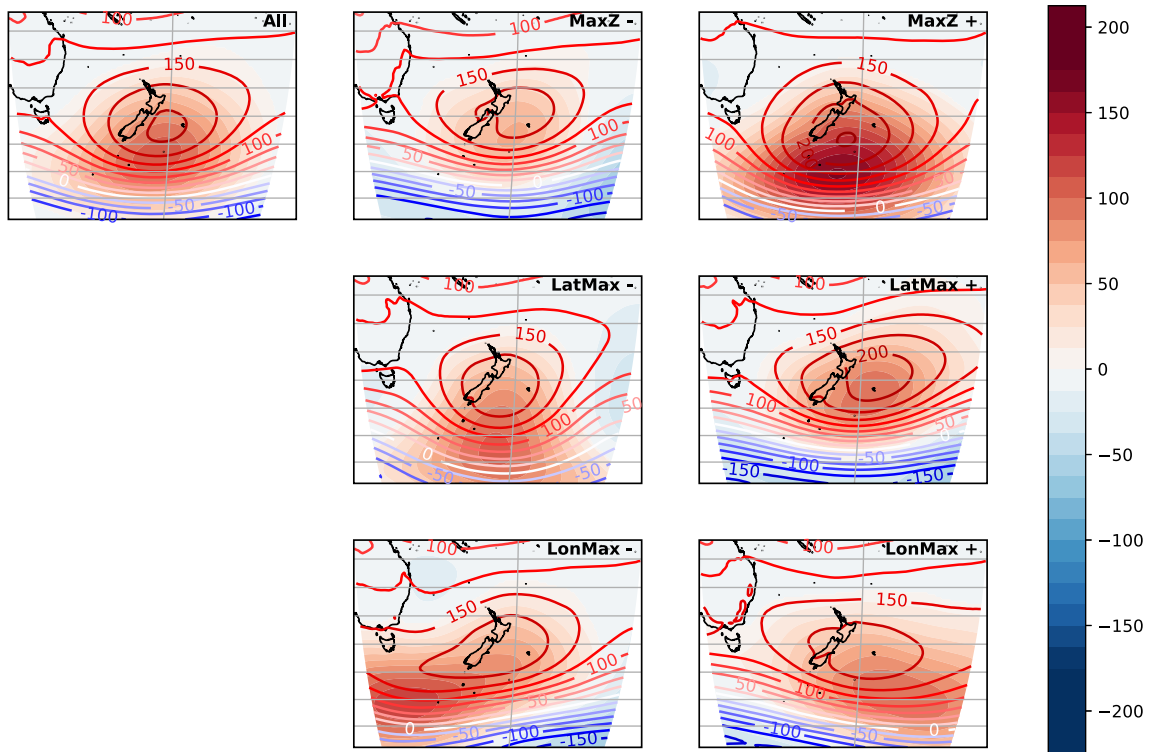


**FIGURE 5** Daily Z1000 raw fields (contours, m: blue means negative, red means positive) and anomalies (see colour bar) associated with the HSE weather type over the period 1979–2019. All: all occurrences of HSE. MaxZ–, MaxZ+: 20% weakest/strongest Z1000 anomalies associated with HSE. LatMax–, LatMax+: 20% southernmost/northernmost location of the Z1000 maximum. LonMax–, LonMax+: 20% westernmost and easternmost longitudes. Anomalies that are not statistically different from the climatology at the 95% level according to a 1-tailed  $t$  test are shaded white [Colour figure can be viewed at [wileyonlinelibrary.com](http://wileyonlinelibrary.com)]

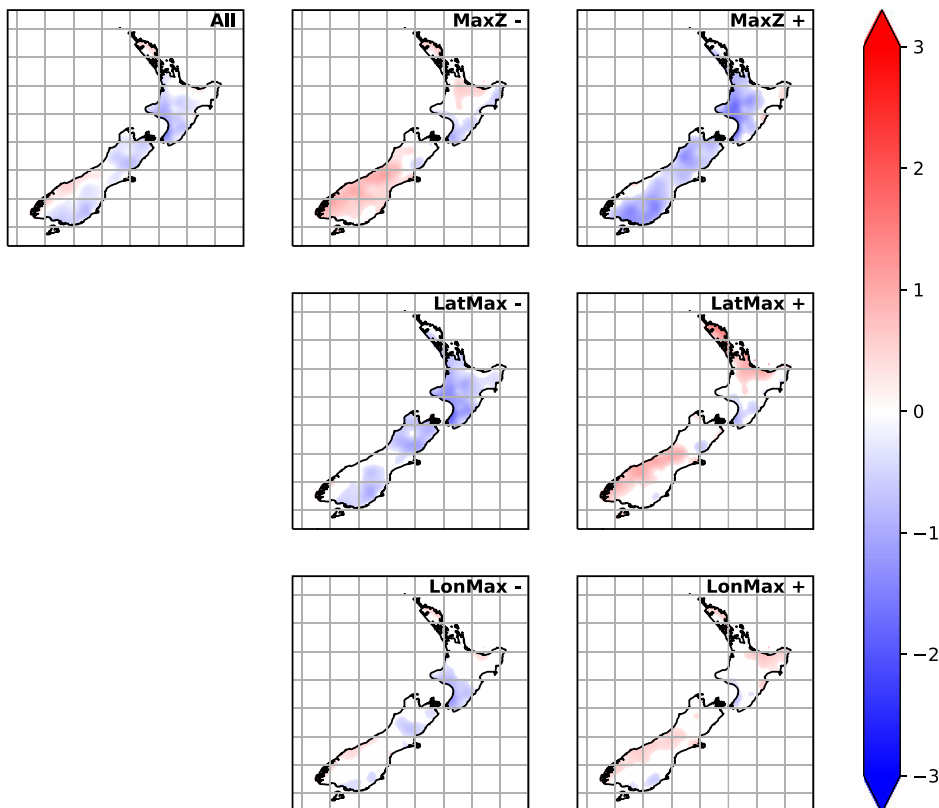
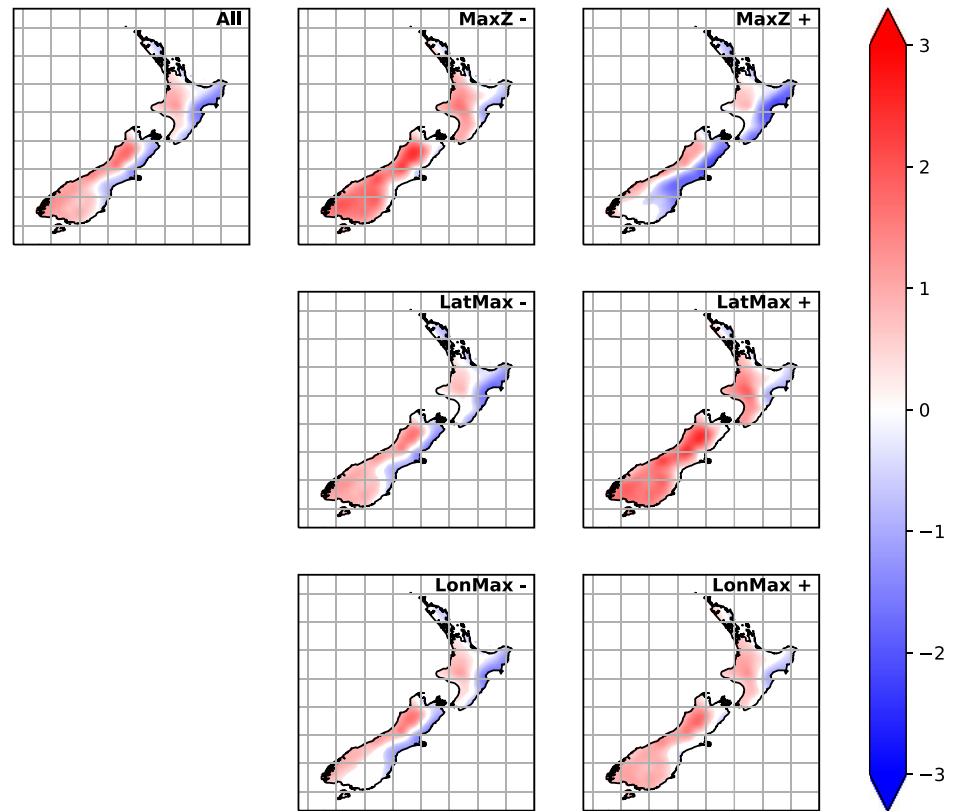


**FIGURE 6** Daily Tn anomalies ( $^{\circ}\text{C}$ : see colour bar) associated with the HSE weather type over ANZ according to VCSN data over the period 1979–2019. Opposite polarities of all ACA metrics extracted as for Figure 5. Anomalies that are not statistically significant at the 95% level according to a 1-tailed  $t$  test are shaded white [Colour figure can be viewed at [wileyonlinelibrary.com](http://wileyonlinelibrary.com)]

**FIGURE 7** Daily Tx anomalies ( $^{\circ}\text{C}$ : see colour bar) associated with the HSE weather type over ANZ according to VCSN data over the period 1979–2019. Opposite polarities of all ACA metrics extracted as for Figure 5. Anomalies that are not statistically significant at the 95% level according to a 1-tailed  $t$  test are shaded white [Colour figure can be viewed at [wileyonlinelibrary.com](http://wileyonlinelibrary.com)]



On average, the HSE type is characterized by an atmospheric ridge located southeast of ANZ, hence its name (Figure 5). Depending on the opposite polarities of its ACA descriptors, it shows a broad variability of daily Z1000' patterns. The intensity of the main ACA is highly variable (from +50 to +300 m compared to the climatology), as are its latitude ( $35^{\circ}$ – $65^{\circ}\text{S}$ ) and longitude (the preferred location being between  $160^{\circ}\text{E}$  and  $170^{\circ}\text{W}$ , with extreme locations extending beyond these values, although only represented in a couple of occurrences: see Figure 5 and P21, their fig. 4). This large spread in the spatial coordinates of the high-pressure ACA implies that its average location southeast of ANZ is likely to change to south or east, from 1 day to another or over a sequence of days. Such variability has strong implications for atmospheric circulation in the region (see section 3.2).

Figures 6 and 7, respectively, show daily minimum and maximum air temperature anomalies in ANZ associated with opposite polarities of these ACA descriptors. On average, HSE is associated with weak (but significant) negative Tn anomalies in ANZ (Figure 6, “All” panel), while Tx anomalies show strong spatial differences, with positive anomalies along the west coast of both North and South Islands, and negative Tx anomalies on their eastern sides (Figure 7, “All” panel). Such average anomalies conceal large variability within WT occurrences. Figure 6 reveals that the sign of Tn anomalies is likely to

change, depending on the characteristics of the high-pressure ACA associated with this type. The strongest ridge events (MaxZ+) and also the southernmost locations of the HSE ridges (LatMax–) yield negative Tn anomalies that are spatially coherent over the country. Although their pattern is quite similar to the average thermal signature of this WT, their magnitude is much stronger. The weakest ridge events and the northernmost locations of the high-pressure ACA are, by contrast, associated with significant positive Tn anomalies, especially over the southwestern parts of the South Island. The longitude of the high-pressure ACA has a weaker effect on modulating Tn, even though westernmost (LonMax–) locations tend to favour weak cold anomalies and easternmost (LonMax+) events yield weak warm anomalies. These signals are of weaker amplitude, extension and significance when compared with the effects of changing latitude and intensity of the ridges.

Figure 7 shows the corresponding results for Tx anomalies. The marked east–west contrast found on average for this WT mostly prevails for the strongest (MaxZ+), and, to a lesser extent, southernmost (LatMax–) and westernmost (LonMax–) locations of the atmospheric high. Opposite aspects of HSE (i.e., the weakest, northernmost or easternmost occurrence of the ridge) tend to favour uniformly positive Tx anomalies

over ANZ, except for localized regions in the eastern part of the North Island.

A few other WT types of K2K also present marked intra-type variability. For the WT types associated with the largest mean temperature anomalies, the properties of ACAs mostly modulate the amplitude and, secondarily, the spatial extension of temperature anomalies across ANZ (not shown). This is the case for both “warm” types (TNW, W, HE, and NE) and “cold” types (SW and HW). Types T and TSW show weaker within-type diversity, thereby suggesting that these WT types lead to more consistent temperature anomalies. The remaining types H, HNW, and R show large internal variability, exhibiting strong similarities with the case of type HSE discussed above. Temperature anomalies associated with these WT types are shown in Figures S6–S11. These results imply that the mere analysis of WT occurrence is not sufficient to explain air temperature variability over ANZ, hence the need to consider within-type diversity by analysing their associated ACAs.

### 3.2 | Mechanisms

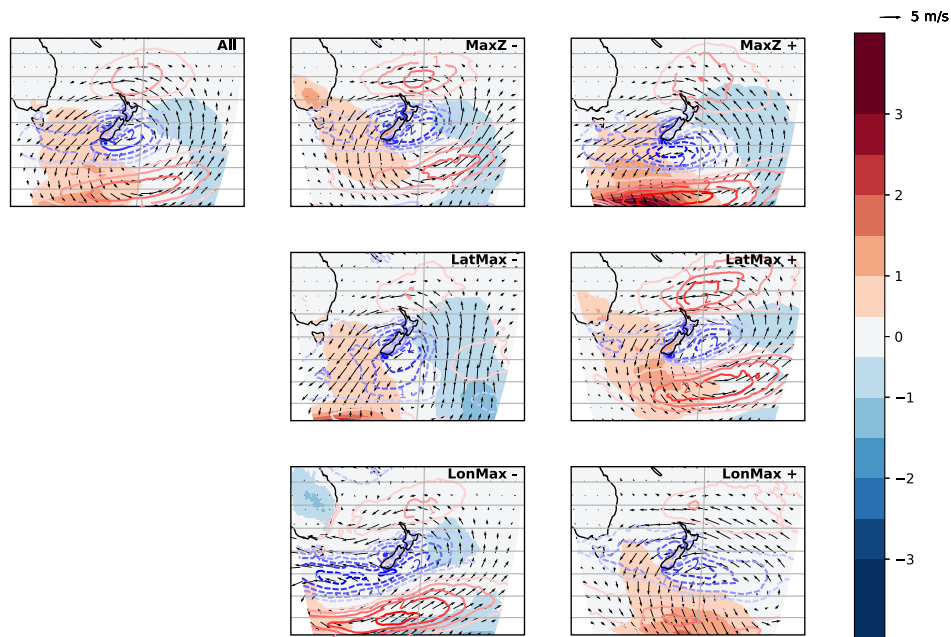
While K2K's 12 WT types have a more spatially uniform influence on  $T_n$  (Figure 3) than the spatially contrasting anomalies of  $T_x$  (Figure 4),  $T_n$  and  $T_x$  anomalies generally tend to be of a similar sign. This denotes large-scale mechanisms influencing air temperature in a similar way across ANZ, thereby suggesting a strong influence of meridional advection of heat (having comparable effects on  $T_n$  and  $T_x$ : e.g., Pohl *et al.*, 2021a). More local processes, such as those associated with radiative exchanges (Ummenhofer and England, 2007; Bony *et al.*, 2015), are primarily modulated by cloud cover (having generally opposite effects on  $T_n$  and  $T_x$ ), but also include the Foehn effect of the main mountain ranges (Sturman and Wanner, 2001). Cloud cover (a) reduces both surface solar radiation during the day (thereby decreasing daily peaks of  $T_x$ ), but also (b) decreases night-time radiative losses under the impact of cloud on longwave radiation flux (thereby promoting warmer  $T_n$  overnight). In the ANZ region, local variations in cloud cover result from uplift of air on the upwind side of the main mountain ranges and descent of air to the lee (Sturman and Wanner, 2001). This effect is clear for the  $T_x$  anomalies associated with the HSE type shown in Figure 7, as anticyclones located southeast of ANZ typically produce cloud cover in northeasterly airflow along the eastern side of the mountains (Sturman and Tapper, 2006), especially when they are strong (MaxZ+), close to ANZ and extend further south (LatMax–).

Figure 8 shows regional-scale near-surface circulation and temperature anomalies associated with type HSE,

according to ERA5. For better readability, Figure S1 presents 2 m air temperature anomalies based on ERA5 over and around ANZ. Figure 9 presents the same results for the mid-troposphere (700 hPa) and also shows surface solar radiation anomalies dependent on the properties of the positive ACA described by this WT. For comparative purposes, Figure S2 shows the same results for all 12 WT types. The role of meridional advection is confirmed, with northerly anomalies bringing warm and humid air from the tropics towards the mid-latitudes, thereby leading to positive temperature anomalies. The opposite is found for southerly anomalies transporting cold dry air from higher latitudes. For type HSE, northerly anomalies are located west of the South Island of ANZ, and southerly anomalies lie to the east, which, together with the orographic effect of the mountains on cloud, rain and temperature via the Foehn effect, help to explain the regional-scale trans-alpine contrasts and the positive temperature anomalies prevailing over western ANZ (Figure 7). The variability in intensity and latitude of the positive ACA associated with type HSE modifies both the strength and direction of regional-scale atmospheric circulation anomalies, thereby having a strong influence on air temperature over ANZ (Figures 8 and 9). Northerly winds are directed towards the land areas (especially the western South Island) when the atmospheric high is either of weak amplitude (MaxZ–) or in its northernmost location (LatMax+), promoting anomalously warm conditions over southwestern ANZ. Opposite features of the atmospheric high-pressure system bring southeasterly anomalies closer, particularly to northeastern ANZ, as well as orographic cloud development along the east coast of both islands, leading to colder conditions (for both  $T_n$  and  $T_x$ , but especially  $T_x$ : Figures 6 and 7).

Changes in cloud fraction (Figure S3) and precipitable water (Figure S4) at the regional scale are of moderate amplitude but significant. There are presumably more fine scale variations over ANZ than can be shown as a result of interaction with the complex topography. However, global reanalyses are probably still too coarse to accurately reproduce such local patterns (hence, small-scale patterns across ANZ are not the scope of this study). Regional-scale changes show slightly decreased cloud cover along the east coasts of ANZ when the atmospheric high pressure is particularly weak (MaxZ–) or when it is located further north (LatMax+: Figure S3). This situation could increase surface solar radiation and contribute to positive  $T_x$  anomalies in the afternoon (Figure 9).

Figures S6–S11 show examples of types R, H, and HNW, which are all associated with particularly large within-type diversity in terms of temperature anomalies across ANZ. Variability of temperature anomalies associated with other WT types is mainly caused by changes in



**FIGURE 8** As for Figure 5, but for 10-m wind anomalies (vectors,  $\text{m}\cdot\text{s}^{-1}$ ), 10-m wind speed anomalies (colour contours,  $\text{m}\cdot\text{s}^{-1}$ : blue means lower and red means higher wind speed than normal) and 2-m air temperature ( $^{\circ}\text{C}$ : see colour bar) anomalies associated with the HSE weather type. Only anomalies that are statistically significant at the 95% level according to a 1-tailed  $t$  test are represented. A zoomed and more readable version of this figure centred on ANZ can be found in Figure S1 [Colour figure can be viewed at [wileyonlinelibrary.com](http://wileyonlinelibrary.com)]

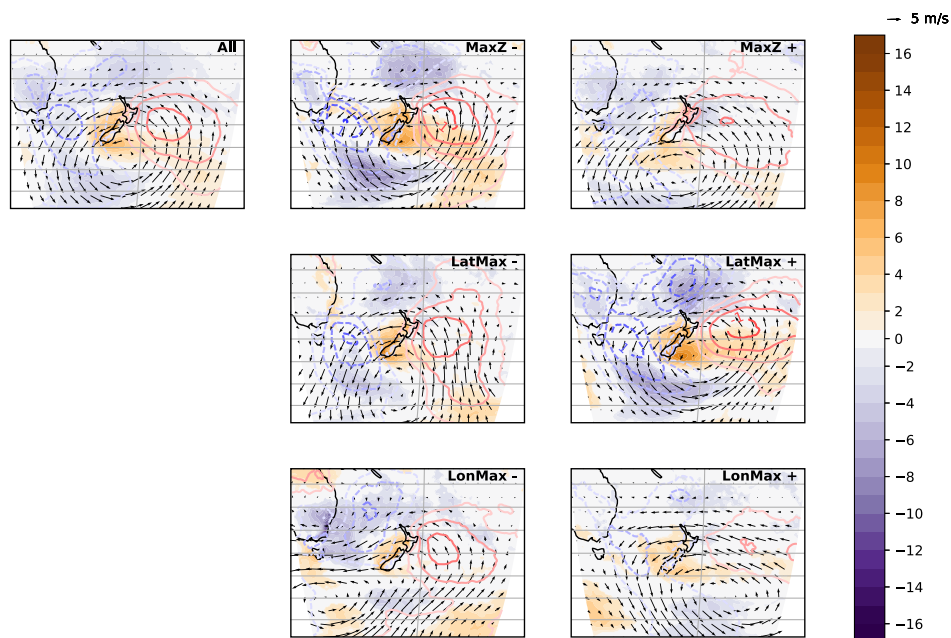


**FIGURE 9** As for Figure 5, but for 700 hPa wind anomalies (vectors,  $\text{m}\cdot\text{s}^{-1}$ ), 2 m specific humidity (colour contours,  $\text{g}\cdot\text{kg}^{-1}$ : blue means wetter and red means drier than normal) and surface solar radiation ( $\text{W}\cdot\text{m}^{-2}$ : see colour bar) anomalies associated with the HSE weather type. Only anomalies that are statistically significant at the 95% level according to a 1-tailed  $t$  test are represented [Colour figure can be viewed at [wileyonlinelibrary.com](http://wileyonlinelibrary.com)]

meridional advection, with air masses reaching ANZ and penetrating inland that cause stronger anomalies than those off the coasts (not shown) to arise. Thus, the

associated mechanisms of surface temperature response to direction of incident flow are in agreement with those discussed above for type HSE.

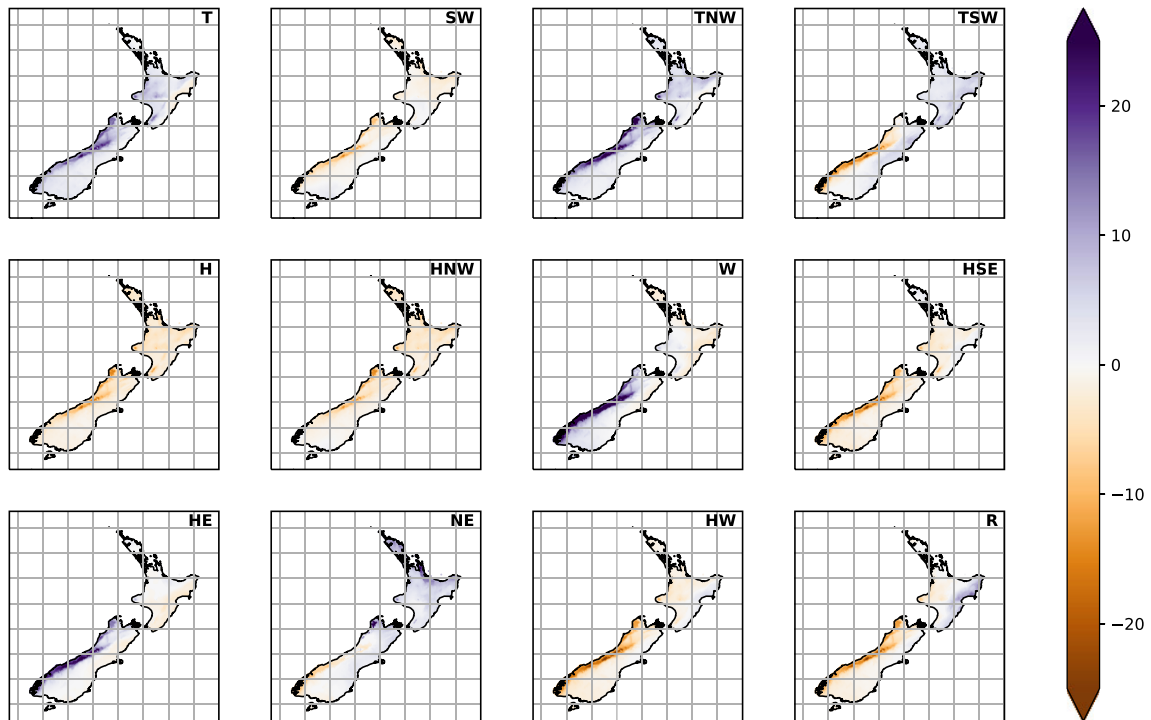


**FIGURE 10** Daily precipitation anomalies (mm: see colour bar) associated with the 12 weather types of Kidson (2000) over the period 1979–2019. Anomalies that are not statistically significant at the 95% level according to a 1-tailed  $t$  test are shaded white [Colour figure can be viewed at [wileyonlinelibrary.com](http://wileyonlinelibrary.com)]

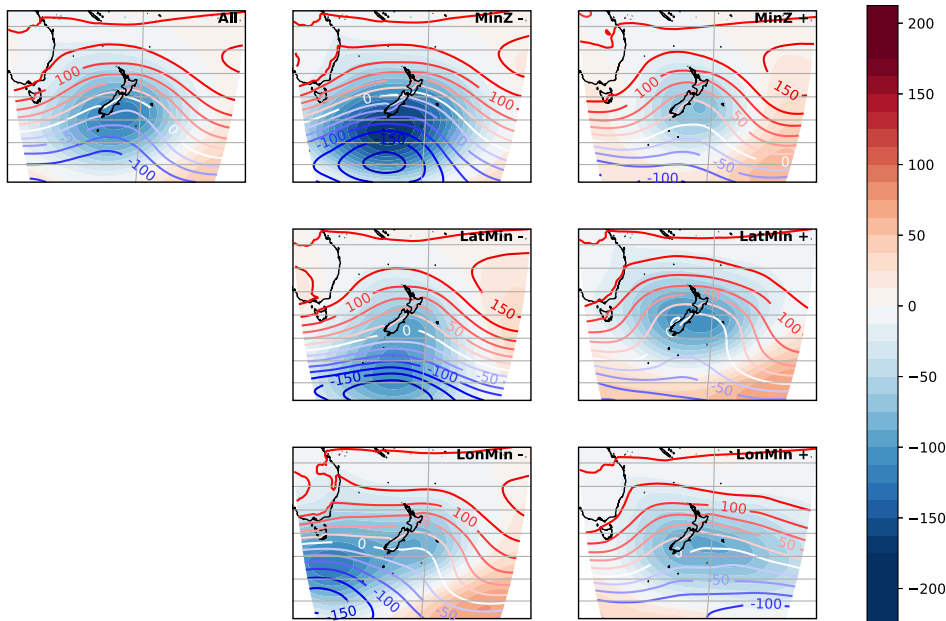


**FIGURE 11** As for Figure 5, but for daily Z1000 raw fields (contours, m: blue means negative, red means positive) and anomalies (m: see colour bar) associated with the T weather type over the period 1979–2019 [Colour figure can be viewed at [wileyonlinelibrary.com](http://wileyonlinelibrary.com)]

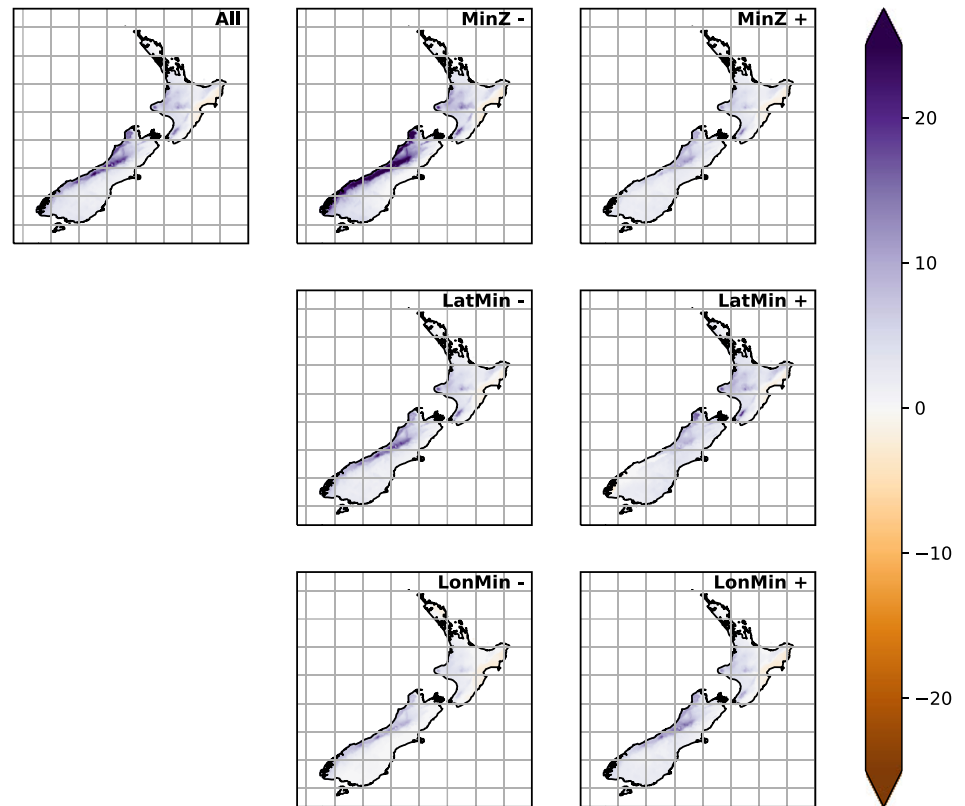
## 4 | DAILY PRECIPITATION ANOMALIES

### 4.1 | Precipitation anomaly patterns

Because precipitation variability associated with the WTs has only been partly discussed in the literature

(Renwick, 2011), Figure 10 presents the inter-type differences in daily precipitation anomalies. Generally, the WTs associated with warm anomalies (Figures 3 and 4) tend also to be associated with anomalously wet conditions. This is due to the poleward transport of heat and moisture from lower latitudes towards the ANZ sector, a result true for most mid-latitude regions (e.g., for the

**FIGURE 12** Daily precipitation anomalies (mm) associated with the T weather type over ANZ according to VCSN data, period 1979–2019. Opposite polarities of all ACA metrics extracted as for Figure 5. Anomalies that are not statistically significant at the 95% level according to a 1-tailed  $t$  test are shaded white [Colour figure can be viewed at [wileyonlinelibrary.com](http://wileyonlinelibrary.com)]



Southern Hemisphere: Pohl *et al.*, 2021a; Udy *et al.*, 2021; Wille *et al.*, 2021). In contrast, WTs that produce cold anomalies also tend to be dry, under the influence of southerly flow favouring incursions of polar air masses towards the mid-latitudes near ANZ (*ibid.*).

Intra-type variability is assessed here using the example of type T (Figure 11). This is the archetype of K2K's “trough” types and the “Low” type according to P21, meaning that it includes only one negative ACA. Hence, three descriptors are used to assess its variability, comprising the intensity (MinZ) and spatial coordinates (LatMin, LonMin) of the regional minimum of Z1000' (Table 1). The canonical anomaly field associated with the T type consists of a well-identified low-pressure ACA located south of ANZ, which promotes strong westerly flow (i.e., anomalously strong westerly wind fields in the mid-latitudes) with a weak southerly component. This average weather situation conceals strong within-type diversity related to the intensity and location of the trough. Thus, the lowest Z1000' is likely to range from nearly  $-400$  to  $-50$  m compared with climatology, but most days show values of between  $-250$  and  $-170$  m (see Figure 4 in P21). Similarly, the latitude of the ACA varies between  $60^{\circ}\text{S}$  and  $30^{\circ}\text{S}$ , although the most recurrent locations typically occur between  $55^{\circ}\text{S}$  and  $45^{\circ}\text{S}$ . Longitudes show an even wider range of values, mostly between  $160^{\circ}\text{E}$  and  $180^{\circ}\text{E}$ . This indicates that, during the occurrence of the “T” type, the main atmospheric low-pressure

system is likely to be located in a broad region encompassing both ANZ itself, but also parts of the Tasman Sea further west, the nearby Pacific Ocean further east, and the Southern Ocean further south.

Figure 12 shows the daily precipitation anomalies associated with these different kinds of “T” type. Anomalously wet conditions are found over the whole country, even though the largest departures from climatology are restricted to the western slopes of the main mountain ranges. This is especially true for the western South Island, due to the major topographic barrier formed by the Southern Alps (Figure 1), where daily precipitation anomalies can reach  $+15$ – $20$  mm at mid-slope, when all occurrences of this WT are considered (Figure 12, “All” panel). This roughly corresponds to a doubling ( $+100\%$ ) of the mean daily amounts there. Although the anomalies are of weaker amplitude over the main topographic features of the North Island, results there confirm the strong exposure effects associated with this type, as western aspects systematically receive the largest precipitation amounts. Although the spatial anomaly pattern remains mostly unchanged within type T, the anomaly amplitudes show large variability. The intensity of the negative ACA has the largest effect: the most negative Z1000' (i.e., the most intense troughs) can produce up to  $+30$  to  $+35$  mm of precipitation along the West Coast region of the South Island with respect to the mean daily climatology ( $+150$ – $175\%$ ). During weaker troughs (MinZ+),

precipitation anomalies along the west coast barely exceed +5 to +7 mm (+25–35%). While the longitude of the ACA modifies the amplitude field only weakly (Figure 12), its latitude has more influence, the southernmost locations tending to bring more moisture towards the western flanks of the main mountains.

Some of the other WTs show comparable within-type variability. Figure S12 presents example of type TNW (see Figure 2), which presents strong similarities with type T as far as associated precipitation anomalies are concerned (Figure 10) but a wider range of possible characteristics depending on its two ACAs, and derived descriptors (Table 1). Figure S13 shows the case of type NE (Figure 2), associated with anomalously wet conditions over the north of ANZ, and dry in the south. Precipitation associated with types SW (generally dry) and HW (opposite to NE) also show strong sensitivity to ACAs, conducive to strong intra-type variability (not shown). By contrast, intra-type diversity is much weaker for dry types H, HSE, and HNW, and spatially contrasting types W and TSW (not shown), meaning that these types are more homogeneous in terms of associated precipitation.

## 4.2 | Mechanisms

Precipitation anomalies in ANZ are strongly driven by advection of moisture towards ANZ (Figure S2). WTs associated with predominant wet anomalies over ANZ (namely T, TNW, W, HE, NE; Figure 10) either show moisture transport from the west (T, W), northwest (TNW), northeast (NE) or north (HE). These circulation anomalies all lead to positive moisture anomalies in the lower troposphere over or around ANZ and, generally, reduced surface solar radiation corresponding to more extensive cloud cover (not shown). By contrast, WTs associated with predominantly dry anomalies over ANZ (namely SW, H, HNW, HSE, HW) coincide with southerly (SW, HW), southwesterly (HNW), or southeasterly (HSE) anomalies advecting dry, cold air from the higher latitudes, or the centre of an atmospheric high (H) promoting clear-sky conditions and atmospheric stability. Finally, types producing strong exposure effects and spatially contrasting precipitation anomalies across ANZ (TSW, R) correspond to a negative ACA centred over ANZ producing northwesterly anomalies in the north and southeasterly anomalies in the south (for TSW) and easterly anomalies almost perpendicular to the main mountains of ANZ, giving thus very strong contrasts between both sides of the main divide.

The interaction between regional-scale atmospheric circulation and finer-scale uplift due to topographic forcing is a key concept to consider in order to understand the spatial distribution of precipitation anomalies across

ANZ. Hence, we estimated the vertical component of the wind (see section 2.3 for details) that is due to the combined influence of the topography and the composite mean wind during all WT occurrences. The types identified as wet in Figure 10 correspond to those showing the largest topographic forcing (Figure S5), with the wet anomalies matching very well to the areas of estimated vertical uplift (negative values in Figure S5). These results confirm that precipitation variability in ANZ may be interpreted as arising from spatial effects that relate to horizontal advection of moisture that is forced to vertically ascend when intersecting mountain slopes. This situation produces stark contrasts for rainfall outcomes on opposite sides of the main divide.

By modulating circulation anomalies, the variability in both the location and intensity of ACAs that are associated with different WTs is likely to modify topographically-forced instabilities which then leads to changes in precipitation anomalies (Figure 12). Figures 13 and 14, respectively, show the regional-scale circulation anomalies and estimated topographic uplift associated with opposite polarities of the descriptors reflecting the internal variability of type T. Qualitatively similar conclusions are reached when considering the case of the other “wet” types (like TNW, W, or HE; not shown). The largest positive precipitation anomalies associated with type T (MinZ– and, to a lesser extent, LatMin–; Figure 12) occur when the airflow generated by the atmospheric Low is perpendicular to the main topographic barrier of the South Island and reaches the more isolated summits of the North Island (Figure 13). This results in an enhanced topographic uplift (Figure 14) that promotes anomalously high precipitation. While it strongly modifies the regional-scale circulation, the longitude of the negative ACA of type T has little influence on the direction and strength of the moisture and momentum fluxes across the main mountains of ANZ (Figures 13 and 14), hence its limited influence on precipitation (Figure 12).

## 5 | DAILY PRECIPITATION AND TEMPERATURE EXTREMES

In this section, we quantify the relative contribution of each WT to extreme precipitation and temperature occurrence, and we assess the extent to which these types (and their main ACAs) change when associated versus not associated with such extremes.

### 5.1 | Precipitation extremes

Extreme precipitation events need further attention because of the damage that they repeatedly cause in ANZ

**FIGURE 13** As for Figure 5, but for 700 hPa wind anomalies (vectors,  $\text{m}\cdot\text{s}^{-1}$ ), 2 m specific humidity (colour contours,  $\text{g}\cdot\text{kg}^{-1}$ ) and surface solar radiation (colours,  $\text{W}\cdot\text{m}^{-2}$ ) anomalies associated with the T weather type. Only anomalies that are statistically significant at the 95% level according to a 1-tailed  $t$  test are represented [Colour figure can be viewed at [wileyonlinelibrary.com](http://wileyonlinelibrary.com)]

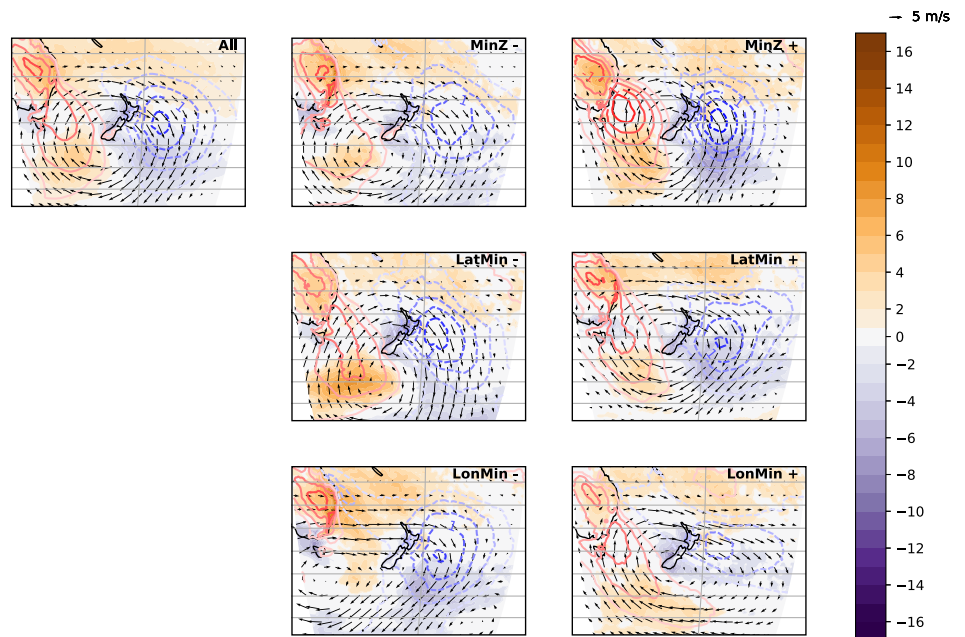
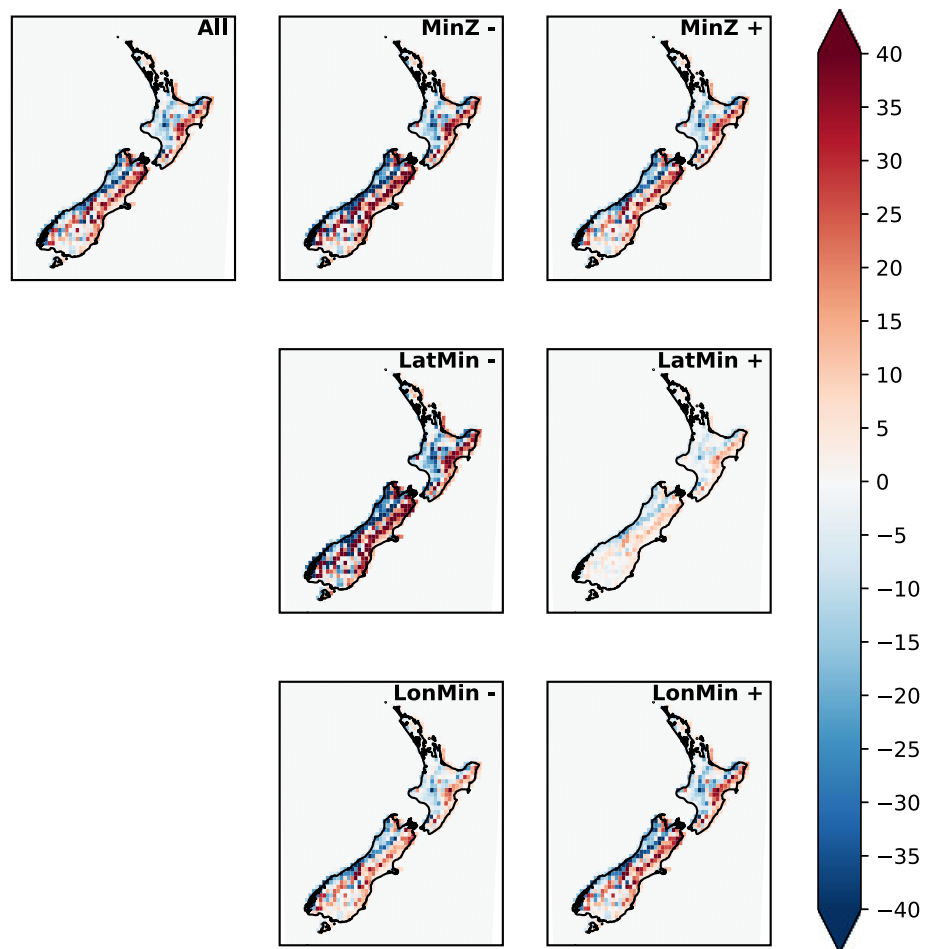


**FIGURE 14** Estimation of the orographic lifting (unitless) associated with the T weather type over ANZ over the period 1979–2019 (see text for details). Negative values mean uplift and positive values denote subsidence. Opposite polarities of all ACA metrics extracted as for Figure 5 [Colour figure can be viewed at [wileyonlinelibrary.com](http://wileyonlinelibrary.com)]



(Kingston *et al.*, 2016; Reid *et al.*, 2021). Given the factors modulating precipitation amounts (section 4.2), especially the strength of circulation anomalies and their

orientation with respect to topographic barriers, we attempt to identify the extent to which daily precipitation extremes are associated with synoptic configurations that



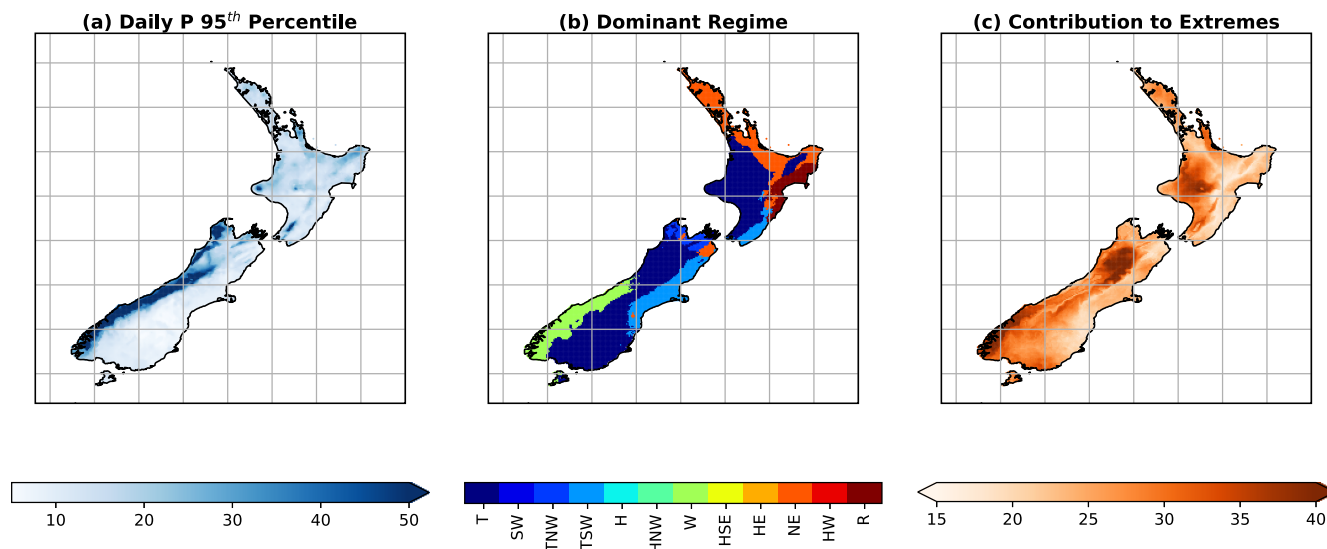


**FIGURE 15** (a) 95th percentile of daily precipitation anomalies (with respect to the mean annual cycle) based on the VCSN dataset. (b) Weather type associated with the largest number of precipitation extremes (daily anomalies above the 95th percentile) for each grid point of the VCSN dataset. (c) Fraction (%) of all precipitation extremes of each grid-point associated with the dominant weather type shown in (b). All analyses are performed on the period 1979–2019 [Colour figure can be viewed at [wileyonlinelibrary.com](http://wileyonlinelibrary.com)]

could deviate (in terms of intensity and/or location of ACAs) from the average situations associated with the original types of K2K.

Figure 15a shows the 95th percentile of the estimated daily precipitation anomalies for each grid-point of the VCSN dataset over ANZ for the period 1979–2019. The spatial distribution is very close to that of the total rainfall (Figure 1), showing that the wettest regions on average are also those with the largest daily departures from the mean. The western slopes of the Southern Alps, facing the dominant westerly winds, receive the most abundant total and extreme precipitation amounts, while the eastern plains and slopes, protected by the topography from prevailing flow, are much drier. These spatial contrasts are particularly marked for intense rainfall, with anomaly values ranging from less than 5 mm per day for the central parts of both South and North Islands, to 50 mm and more (the maximum value being +140 mm compared to climatology) along the west coast of the South Island and for the main mountainous regions of the North Island (Figure 15a). Given the respective climatology of these regions, the 95th percentile of daily precipitation anomalies correspond to regionally-varying daily amounts spanning from 6 to 182 mm. For comparative purposes, the largest daily amounts received over the 1979–2019 period range between 51 and 1,193 mm, from one region of ANZ to another. While it offers a continuous picture of daily rainfall fields at high resolution, the VCSN database has also been shown to produce larger errors for high precipitation amounts, especially in regions with steep topography (Tait *et al.*, 2012; Mason

*et al.*, 2017). Thus, the values cited above should be taken with care, the general coherence of the precipitation fields and the general order of magnitude of the anomalies being more meaningful than the individual values themselves.

Figure 15b shows which WTs are responsible for the largest number of extreme events, identified here as in Figure 15a, for each grid-point of the VCSN dataset. Weather type T, previously discussed as producing anomalously wet conditions across ANZ (Figure 10), cause the largest number of intense to extreme precipitation days over most of the South Island. This includes the northern part of the West Coast region, but also regions east of the main divide, such as Otago and Southland, as well as significant areas of the North Island (especially central and western regions, but also more localized western slopes of mountains in the northeast). In other regions, the WTs having the largest contribution to intense and extreme precipitation days are those that are generally anomalously wet there on average (Figure 10), due to circulation anomalies leading to moisture transport towards these areas (Figure S2). This is, for instance, the case for type “W” in the Fiordland region (southwest of the South Island), “TSW” for most of the Canterbury Plains (and eastern and northeastern parts of the South Island), “NE” for the Northland region (the northern section of the North Island), and “R” for Hawke’s Bay (eastern parts of the North Island). Hence, depending on the exposure of the local terrain, very different synoptic conditions can cause extreme precipitation events in different parts of ANZ.

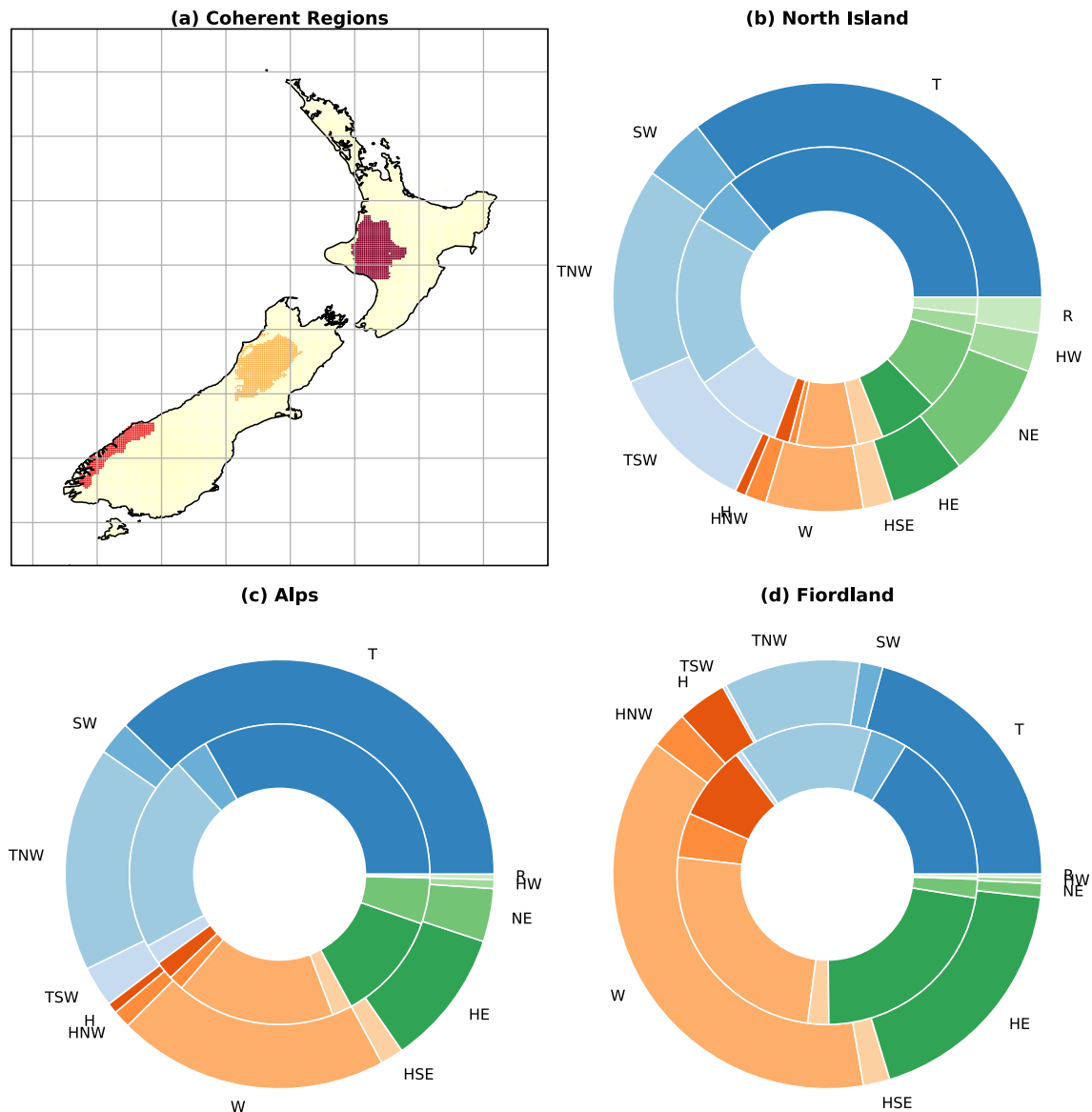


**FIGURE 16** Coherent climate regions for extreme precipitation analysis, and their associations with different weather types. (a) Three coherent regions of rainfall extremes (see text for details). (b–d) The relative contribution of all 12 WTs to precipitation extremes for each region shown on the map. The inner circle corresponds to NCEP/NCAR weather type distribution, and the outer circle to the ERA5 re-definition. All analyses are based on the VCSN dataset over the period 1979–2019 [Colour figure can be viewed at [wileyonlinelibrary.com](https://onlinelibrary.wiley.com)]

Nonetheless, Figure 15c shows that, in most regions, the overall contribution of these dominant WTs to precipitation extremes remains moderate. Generally, 15–35% of the extremes are associated with the dominant WTs identified in Figure 15b. This could be due to interferences with other rain-bearing systems or mechanisms not necessarily discriminated by the WTs, like atmospheric rivers (recently shown to be involved in many major rain events in ANZ: Prince *et al.*, 2021; Reid *et al.*, 2021; Shu *et al.*, 2021), or ex-tropical cyclones (Lorrey *et al.*, 2014b). Three main regions show slightly larger values, denoting a stronger relationship between WTs and intense or

precipitation extremes: (a) the Fiordland region, southwest of the South Island; (b) the northern part of the Southern Alps in the South Island; (c) the central-western part of the North Island, around the volcanic peak of Mount Ruapehu. These three regions are further analysed in Figure 16. Here, we select the areas where the contribution of the dominant WT exceeds 30% and calculate regional precipitation indices over the three delineated regions shown in Figure 16a. For each region, the relative contribution of all 12 WTs to intense to extreme events is then represented as pie plots (Figure 16b–d). The analysis is done for both the original

WT time distribution, based on NCEP/NCAR reanalysis, and the updated ERA5 redefinition, as results show non-negligible reanalysis-dependency.

The predominant contribution of type T to intense to extreme events in the central North Island and Southern Alps region is confirmed for both reanalyses. Other WTs strongly associated with intense events vary between these two regions, and show stronger sensitivity to the reanalysis upon which they are based. For the North Island area, types TNW, TSW, and NE are each associated with at least 15% of the extreme events, while regime W provides about another 10%. All these WTs, wet on average over each region (Figure 10), are responsible for a larger proportion of extremes in the ERA5 re-definition than in the original NCEP/NCAR definition of the types. This means that all other WTs have a weaker influence on extremes according to their updated ERA5 time distribution. Quite similar results are obtained with the Southern Alps area, except that types W and HE coincide with a larger number of intense to extreme events occurring there, while types TSW and NE are of much less importance. Once again, the types associated most frequently with high daily precipitation are those that are wet on average over the region, and more generally, over the whole West Coast region of the South Island. Finally, extreme precipitation for Fiordland has a strong association with WTs. In that region, the W type is clearly the predominant synoptic driver for heavy rainfall anomalies, especially according to the ERA5 time distribution. The following WTs are, by decreasing contribution, T, HE and TNW (according to ERA5) or HE, T, and TNW (according to NCEP/NCAR). Types that show very weak contribution to extremes in other regions (like H and HNW) show diminished, but non-negligible association with high precipitation events in the southwestern tip of ANZ. While often associated with dry anomalies further north, these types correspond, on average, to near-climatology conditions in Fiordland. This shows how important within-type variability may be, with a type associated with near-climatological conditions on average frequently leading to climate extremes.

This leads us to investigate what differentiates days that are and are not associated with an intense or extreme precipitation event within the same WT. To do this we create two samples of days for each region, by selecting the predominant WTs (T for central North Island and Southern Alps, W for Fiordland) that were associated and not associated with a daily precipitation amount exceeding the local 95th percentile. ACA descriptors associated with these types are then compared using 2-tailed *t* tests at the 95 and 99% confidence levels.

For all three regions shown in Figure 16, the intensity of the negative ACA associated with the corresponding

types is systematically different between these two samples. Extreme precipitation days correspond to atmospheric troughs that are significantly more intense (at the 99% level) than the other days in the same WT, but with lower (nonextreme) precipitation. This is indicative of a subclass of mid-latitude cyclones that are seemingly stronger than usual relative to a category of synoptic systems that have similar general geopotential height patterns. For instance, for the Southern Alps region, the median intensity of negative ACAs associated with heavy precipitation is  $-250$  m (with a standard deviation of 40 m) compared to climatology, versus only  $-200 \pm 40$  m for nonintense precipitation days, leading to a statistically significant difference. This result is verified for both the original NCEP/NCAR definition of WTs, and the ERA5 update (not shown). Anomalously strong cyclones (see, e.g., Figure 11, for type T) promote stronger moisture transport towards ANZ (Figure 13), which generates stronger topographic uplift (Figure 14) leading to very large precipitation amounts (Figure 12).

All other descriptors show nonsignificant differences between intense and weaker precipitation samples except for the North Island, where the lower latitude cyclone location favours larger precipitation amounts and anomalies above the 95th percentile. The northern locations of some troughs are also conducive to a northward shift of associated moisture advection that reaches the west coast of the North Island ahead of the west coast of the South Island. The nonsignificance of results concerning all other ACA descriptors confirm that intense and extreme daily precipitation can occur in ANZ from many different synoptic conditions, a result verified both between and within WTs.

## 5.2 | Temperature extremes

In Supporting Information, we duplicated these analyses for extreme anomalies of  $T_n$  and  $T_x$ , which is an issue of increasing importance that we need to understand in order to attribute the causes of extreme temperatures over a region. A weaker relationship is observed between temperature extremes and the WTs. Extremes in  $T_n$  are most often recorded during occurrences of the W (TNW and NE) types over the South (North) Island (Figures S14 and S15). Extremes in  $T_x$  relate to the HSE over a large fraction of both islands, especially their western parts, while results are less clear and more contrasting along the east coast (Figures S16 and S17). WT sequences that are associated with temperature extremes also show quite weak differentiation from more moderate temperature occurrences. The main result indicates a weaker ACA for the type sequences leading to  $T_x$  extremes, thereby

leading to anomalously weak horizontal advection over ANZ (not shown). This situation could promote a stronger (weaker) land (oceanic) influence, due to lighter winds and less mixing, and favour larger temperature increases over land during the day, causing therefore strong positive Tx anomalies.

## 6 | DISCUSSION AND CONCLUSION

One of the main limitations of weather types (WTs) is that they discretize continuous climate variability into a small number of categories, whose representativity may be questioned. To address this concern, in P21, we defined descriptors used to infer within-type variability, by quantifying the basic properties (intensity, location) of the main atmospheric centres of action (ACAs) associated with these WTs. Here, we build upon that work and attempt to analyse the dependency of local climate variables (daily precipitation amounts, minimum and maximum air temperature) on regional-scale WTs over a region characterized by complex topography that strongly interacts with atmospheric circulation, Aotearoa New Zealand (ANZ).

The relationships between regional-scale WTs and the local-scale climate appear more complex than previously demonstrated (e.g., K2K; Jiang, 2011; Renwick, 2011; Jiang *et al.*, 2013a; Gibson *et al.*, 2016). WTs conceal strong within-type diversity, implying that the mere analysis of WT occurrence is not sufficient to explain daily precipitation and air temperature variability across ANZ. ACA diversity (i.e., their most extreme spatial coordinates, and their strongest or weakest intensities, as monitored by the descriptors of P21) has strong implications for these surface variables, due to their major role for shaping and modifying regional-scale atmospheric circulation. Depending on these characteristics, the magnitude and in some cases, the sign of local-scale climate variables can be significantly modified. While the effects of a given WT are more stable in time when they are of strong magnitude (for instance, dry conditions under anticyclonic conditions), within-type variability leads to major changes in the magnitude and spatial distribution of climate anomalies when the latter are of weaker amplitude, and/or spatially contrasting. In ANZ, this is mostly the case for WTs associated with strong exposure effects, with surface and atmosphere weather patterns of opposite sign occurring on either side of the main mountain ranges.

Dominant mechanisms linking regional-scale WTs to local-scale climate variability involve adjustment of

atmospheric circulation to the intensity and location of the main ACA over and near ANZ, as follows:

1. Meridional advection of warm and moist air from lower latitudes or cold and dry air masses from higher latitudes that drive the major component of temperature variability; with finer-scale processes such as cloud cover having a secondary, yet non-negligible impact.
2. Orographic lifting resulting from lower-tropospheric circulation anomalies interacting with the main topographic features of ANZ, which results in uplift and wet conditions on windward slopes, and dry and warm conditions promoted by Foehn effect on the leeward side of the ranges.

Because of significant impacts on local society, environment, and infrastructure, we also considered the case of intense to extreme precipitation events defined as days exceeding the 95th percentile of daily precipitation anomalies. From one region of ANZ to another, this corresponds to daily rainfall amounts ranging from 6 to 182 mm. The relative contribution of WTs to intense and extreme events varies from one region to another. In most areas, intense to extreme events are likely to occur from at least two and up to four WTs, thereby showing that a range of synoptic conditions can cause major precipitation events in the region. Nonetheless, a common pattern across ANZ is that such events clearly coincide with negative ACAs (i.e., cyclonic conditions) that are significantly stronger than usual. Such intense mid-latitude cyclones favour particularly strong incident flow, maximizing moisture advection and promoting heavy precipitation in the most exposed regions and on windward slopes. Associations between WTs and extreme temperature is generally weaker than for precipitation extremes.

By showing that the relationship between local climate and WTs is not as obvious as often assumed, and that within-type variability is strong at both synoptic and local scales, this study also suggests that studies based on analogues should be careful when considering whether similar WT occurrence can directly translate into similar local climate conditions. The descriptors for monitoring ACAs used here may help improve such analyses, either by selecting more similar synoptic contexts, or by deliberately considering contrasting configurations related to modes of variability. In the latter case, however, one should expect strongly varying surface climate anomalies resulting from interactions between regional-scale atmospheric dynamics, thermodynamics, and local-scale topography.

Such approaches linking synoptic-scale WTs to local climate conditions are also important for assessing possible impacts on human activities such as agriculture and for developing adaptation strategies in response to projected future climates. Sturman and Quénol (2013) studied the relationship between changes in atmospheric circulation in ANZ and observed trends in temperature and frost events using K2K's WT classification for the period 1958–2010. They identified an increase in frost events associated with more frequent clear skies along the east coast of the country, resulting from changes in weather patterns (more frequent highs, fewer low-pressure systems, stronger zonal and southerly flows). Meanwhile, significant positive trends were found in the latitude of atmospheric ridges (P21), possibly denoting a poleward expansion of the Hadley circulation (Lu *et al.*, 2007; Hu *et al.*, 2011; Tao *et al.*, 2016; Nguyen *et al.*, 2018), with a southward extension of stable conditions from the subtropics towards the mid-latitudes. However, the existence and significance of such trends needs to be assessed over longer time periods, in order to increase the robustness of the conclusions. Such analyses could be based either (a) on long-term ensemble reanalyses (e.g., the 20th Century Reanalyses: Slivinski *et al.*, 2020, or ERA-20C: Poli *et al.*, 2016), or (b) on long observational time series of weather stations, available since the late 19th or early 20th centuries, to overcome the difficulties associated with the much shorter time coverage of the VCSN data used in this work. Over even longer time periods, reconstructions performed for the Holocene (Lorrey *et al.*, 2007; 2008; Ackerley *et al.*, 2011; 2013; Lorrey *et al.*, 2012; 2014a; Prebble *et al.*, 2017) could help establish the local effects of larger-scale climate variability, evolution and change in the southern mid-latitude dynamics. The results discussed here highlight the importance of multiscale approaches (in both time and space) to define the spatial variability of climate at the local scale in relation to synoptic-scale WTs.

More generally, the approaches presented in this study could be applied to assess the regional-to-local effects of climate change in more detail. High priority should be given to disentangling long-term changes in the atmospheric dynamics of the Southern Hemisphere (i.e., transient variability and storm tracks in the southern mid-latitudes). Such changes may result from stratospheric ozone recovery or the increasing greenhouse effect caused by anthropogenic activities, as well as local-scale conditions arising from synoptic-scale extension, which are expected to change because of warmer and moister air masses that modify both precipitation and temperature. Such in-depth assessment is critical to allow regions to understand the impacts of extreme weather

and climate regimes and to better adapt to ongoing climate change.

## AUTHOR CONTRIBUTIONS

**Benjamin Pohl:** Conceptualization; methodology; software; formal analysis; visualization; writing. **Andrew Sturman:** Formal analysis; writing. **James Renwick:** Formal analysis; writing. **Hervé Quénol:** Formal analysis; writing; funding acquisition. **Nicolas Fauchereau:** Resources; methodology; data curation. **Andrew Lorrey:** Writing; formal analysis; funding acquisition. **Julien Pergaud:** Resources; data curation.

## ACKNOWLEDGEMENTS

This study is a contribution to the International Research Programme VinAdapt funded by France and New Zealand, and sea4seas project funded by the Université de Bourgogne. Andrew Lorrey and Nicolas Fauchereau were supported by the NIWA Strategic Science Investment Fund project “Climate Present and Past.” All analyses were made with Python (numpy, pandas, scipy, sklearn, math, matplotlib, cartopy, seaborn, and netCDF4), the developers of which are thanked. Two anonymous reviewers are thanked for their constructive comments that helped improve the text and the figures of this article. Calculations were performed using HPC resources from DNUM CCUB (Centre de Calcul de l'Université de Bourgogne).

## ORCID

Benjamin Pohl  <https://orcid.org/0000-0002-9339-797X>

## REFERENCES

- Ackerley, D., Lorrey, A., Renwick, J., Phipps, S., Wagner, S., Dean, S., Singarayer, J., Valdes, P., Abe-Ouchi, A., Ohgaito, R. and Jones, J. (2011) Using synoptic type analysis to understand New Zealand climate during the Mid-Holocene. *Climate of the Past*, 7(4), 1189–1207. <https://doi.org/10.5194/cp-7-1189-2011>.
- Ackerley, D., Lorrey, A., Renwick, J., Phipps, S.J., Wagner, S. and Fowler, A. (2013) High-resolution modelling of the New Zealand climate during the Mid-Holocene. *Holocene*, 23, 1272–1285. <https://doi.org/10.1177/0959683613484612>.
- Bony, S., Stevens, B., Frierson, D.M.W., Jakob, C., Kageyama, M., Pincus, R., Shepherd, T.G., Sherwood, S.C., Siebesma, A.P., Sobel, A.H., Watanabe, M. and Webb, M.J. (2015) Clouds, circulation and climate sensitivity. *Nature Geoscience*, 8(4), 261–268. <https://doi.org/10.1038/ngeo2398>.
- Cassou, C., Terray, L., Hurrell, J.W. and Deser, C. (2004) North Atlantic winter climate regimes: spatial asymmetry, stationarity with time, and oceanic forcing. *Journal of Climate*, 17, 1055–1068.
- Champagne, O., Pohl, B., McKenzie, S., Buoncristiani, J.F., Bernard, E., Joly, D. and Tolle, F. (2019) Atmospheric circulation modulates the spatial variability of temperature in the

- Atlantic–Arctic region. *International Journal of Climatology*, 39(8), 3619–3638. <https://doi.org/10.1002/joc.6044>.
- Cullen, N.J., Gibson, P.B., Mölg, T., Conway, J.P., Sirguey, P. and Kingston, D.G. (2019) The influence of weather systems in controlling mass balance in the Southern Alps of New Zealand. *Journal of Geophysical Research: Atmospheres*, 124(8), 4514–4529. <https://doi.org/10.1029/2018JD030052>.
- Eden, J.M., Widmann, M., Maraun, D. and Vrac, M. (2014) Comparison of GCM- and RCM-simulated precipitation following stochastic postprocessing. *Journal of Geophysical Research: Atmospheres*, 119, 11040–11053. <https://doi.org/10.1002/2014JD021732>.
- Fauchereau, N., Pohl, B. and Lorrey, A. (2016) Extratropical impacts of the Madden–Julian oscillation over New Zealand from a weather regime perspective. *Journal of Climate*, 29(6), 2161–2175. <https://doi.org/10.1175/JCLI-D-15-0152.1>.
- Fauchereau, N., Pohl, B., Reason, C.J.C., Rouault, M. and Richard, Y. (2009) Recurrent daily OLR patterns in the southern Africa/southwest Indian Ocean region, implications for South African rainfall and teleconnections. *Climate Dynamics*, 32(4), 575–591. <https://doi.org/10.1007/s00382-008-0426-2>.
- Gibson, P.B., Perkins-Kirkpatrick, S.E. and Renwick, J.A. (2016) Projected changes in synoptic weather patterns over New Zealand examined through self-organizing maps. *International Journal of Climatology*, 36, 3934–3948. <https://doi.org/10.1002/joc.4604>.
- Hersbach, H., Bell, B., Berrisford, P., Hirahara, S., Horányi, A., Muñoz-Sabater, J., Nicolas, J., Peubey, C., Radu, R., Schepers, D., Simmons, A., Soci, C., Abdalla, S., Abellan, X., Balsamo, G., Bechtold, P., Biavati, G., Bidlot, J., Bonavita, M., De Chiara, G., Dahlgren, P., Dee, D., Diamantakis, M., Dragani, R., Flemming, J., Forbes, R., Fuentes, M., Geer, A., Haimberger, L., Healy, S., Hogan, R.J., Hólm, E., Janisková, M., Keeley, S., Laloyaux, P., Lopez, P., Lupu, C., Radnoti, G., de Rosnay, P., Rozum, I., Vamborg, F., Villaume, S. and Thépaut, J.N. (2020) The ERA5 global reanalysis. *Quarterly Journal of the Royal Meteorological Society*, 146(730), 1999–2049. <https://doi.org/10.1002/qj.3803>.
- Hu, Y., Zhou, C. and Liu, J. (2011) Observational evidence for poleward expansion of the Hadley circulation. *Advances in Atmospheric Sciences*, 28(1), 33–44. <https://doi.org/10.1007/s00376-010-0032-1>.
- Jiang, N. (2011) A new objective procedure for classifying New Zealand synoptic weather types during 1958–2008. *International Journal of Climatology*, 31(6), 863–879. <https://doi.org/10.1002/joc.2126>.
- Jiang, N., Dirks, K.N. and Luo, K. (2013a) Classification of synoptic weather types using the self-organising map and its application to climate and air quality data visualisation. *Weather and Climate*, 33, 52–75. <https://doi.org/10.2307/26169737>.
- Jiang, N., Griffiths, G. and Lorrey, A. (2013b) Influence of large-scale climate modes on daily synoptic weather types over New Zealand. *International Journal of Climatology*, 33(2), 499–519. <https://doi.org/10.1002/joc.3443>.
- Jiang, N., Hay, J. and Fisher, G. (2004) Classification of New Zealand synoptic weather types and relation to the Southern Oscillation Index. *Weather and Climate*, 23, 3–23. <https://doi.org/10.2307/26169666>.
- Kidson, J.W. (2000) An analysis of New Zealand synoptic types and their use in defining weather regimes. *International Journal of Climatology*, 20, 299–316.
- Kidston, J., Renwick, J.A. and McGregor, J. (2009) Hemispheric-scale seasonality of the Southern Annular Mode and impacts on the climate of New Zealand. *Journal of Climate*, 22(18), 4759–4771. <https://doi.org/10.1175/2009JCLI2640.1>.
- Kingston, D.G., Lavers, D.A. and Hannah, D.M. (2016) Floods in the Southern Alps of New Zealand: the importance of atmospheric rivers. *Hydrological Processes*, 30(26), 5063–5070. <https://doi.org/10.1002/hyp.10982>.
- Kyriakidis, P.C., Kim, J. and Miller, N.L. (2001) Geostatistical mapping of precipitation from rain gauge data using atmospheric and terrain characteristics. *Journal of Applied Meteorology*, 40, 1855–1877.
- Lorrey, A., Fowler, A.M. and Salinger, J. (2007) Regional climate regime classification as a qualitative tool for interpreting multi-proxy palaeoclimate data spatial patterns: a New Zealand case study. *Palaeogeography, Palaeoclimatology, Palaeoecology*, 253(3–4), 407–433. <https://doi.org/10.1016/j.palaeo.2007.06.011>.
- Lorrey, A.M., Fauchereau, N., Stanton, C., Chappell, P.R., Phipps, S.J., Mackintosh, A., Renwick, J.A. and Fowler, A.M. (2014a) The Little Ice Age climate of New Zealand reconstructed from Southern Alps cirque glaciers: a synoptic type approach. *Climate Dynamics*, 42, 3039–3060. <https://doi.org/10.1077/s00382-013-1876-8>.
- Lorrey, A.M., Griffiths, G.M., Fauchereau, N., Chappell, P., Diamond, H.J. and Renwick, J. (2014b) An ex-tropical cyclone climatology for Auckland, New Zealand. *International Journal of Climatology*, 34, 1157–1168. <https://doi.org/10.1002/joc.3753>.
- Lorrey, A.M., Vandergoes, M., Almond, P., Renwick, J., Stevens, T., Bostock, H., Mackintosh, A., Newnham, R., Williams, P.W., Ackerley, D., Neil, H. and Fowler, A.M. (2012) Palaeocirculation across New Zealand during the last glacial maximum at ~21ka. *Quaternary Science Reviews*, 36, 189–213.
- Lorrey, A.M., Williams, P.W., Salinger, J., Martin, T.J., Fowler, A.M., Zhao, J.-X., and Neil, H. 2008. Speleothem stable isotope records interpreted within a multi-proxy framework and implications for New Zealand palaeoclimate reconstruction. *Quaternary International* 187, 52–75.
- Lu, J., Vecchi, G.A. and Reichler, T. (2007) Expansion of the Hadley cell under global warming. *Geophysical Research Letters*, 34(6), L06805. <https://doi.org/10.1029/2006GL028443>.
- Mason, E.G., Salekin, S. and Morgenroth, J.A. (2017) Comparison between meteorological data from the New Zealand National Institute of Water and Atmospheric Research (NIWA) and data from independent meteorological stations. *New Zealand Journal of Forestry Science*, 47, 7. <https://doi.org/10.1186/s40490-017-0088-0>.
- McCauley, M.P. and Sturman, A.P. (1999) A study of orographic blocking and barrier wind development upstream of the Southern Alps, New Zealand. *Meteorology and Atmospheric Physics*, 70(3–4), 121–131. <https://doi.org/10.1007/s007030050029>.
- Michelangeli, P.-A., Vautard, R. and Legras, B. (1995) Weather regimes: recurrence and quasi stationarity. *Journal of the Atmospheric Sciences*, 52(8), 1237–1256.
- Morel, B., Pohl, B., Richard, Y., Bois, B. and Bessafi, M. (2014) Regionalizing rainfall at very high resolution over La Réunion

- Island using a regional climate model. *Monthly Weather Review*, 142, 2665–2686. <https://doi.org/10.1175/MWR-D-14-00009.1>.
- Moron, V., Oueslati, B., Pohl, B. and Janicot, S. (2018) Daily weather types in February–June (1979–2016) and temperature variations in tropical North Africa. *Journal of Applied Meteorology and Climatology*, 57(5), 1171–1195. <https://doi.org/10.1175/JAMC-D-17-0105.1>.
- Nguyen, H., Hendon, H.H., Lim, E.P., Boschat, G., Maloney, E. and Timbal, B. (2018) Variability of the extent of the Hadley circulation in the southern hemisphere: a regional perspective. *Climate Dynamics*, 50(1–2), 129–142. <https://doi.org/10.1007/s00382-017-3592-2>.
- Parsons, S., McDonald, A.J. and Renwick, J.A. (2014) The use of synoptic climatology with general circulation model output over New Zealand. *International Journal of Climatology*, 34(12), 3426–3439. <https://doi.org/10.1002/joc.3919>.
- Pepler, A., Dowdy, A. and Hope, P. (2019) A global climatology of surface anticyclones, their variability, associated drivers and long-term trends. *Climate Dynamics*, 52(9–10), 5397–5412. <https://doi.org/10.1007/s00382-018-4451-5>.
- Pepler, A.S., Di Luca, A. and Evans, J.P. (2018) Independently assessing the representation of midlatitude cyclones in high-resolution reanalyses using satellite observed winds. *International Journal of Climatology*, 38(3), 1314–1327. <https://doi.org/10.1002/joc.5245>.
- Pohl, B., Dieppois, B., Crétat, J., Lawler, D. and Rouault, M. (2018) From synoptic to interdecadal variability in Southern African rainfall: toward a unified view across time scales. *Journal of Climate*, 31, 5845–5872. <https://doi.org/10.1175/JCLI-D-17-0405.1>.
- Pohl, B. and Fauchereau, N. (2012) The Southern Annular Mode seen through weather regimes. *Journal of Climate*, 25(9), 3336–3354. <https://doi.org/10.1175/JCLI-D-11-00160.1>.
- Pohl, B., Lorrey, A., Sturman, A., Quénol, H., Renwick, J., Fauchereau, N. and Pergaud, J. (2021a) “Beyond Weather Regimes”: descriptors monitoring atmospheric centers of action. A case study for Aotearoa New Zealand. *Journal of Climate*, 34, 8341–8360. <https://doi.org/10.1175/JCLI-D-21-0102.1>.
- Pohl, B., Morel, B., Barthe, C. and Bousquet, O. (2016) Regionalizing rainfall at very high resolution over La Réunion Island: a case study for tropical cyclone Ando. *Monthly Weather Review*, 144(11), 4081–4099. <https://doi.org/10.1175/MWR-D-15-0404.1>.
- Pohl, B., Saucède, T., Favier, V., Pergaud, J., Verfaillie, D., Féral, J.-P., Krasniqi, Y. and Richard, Y. (2021b) Recent climate variability around the Kerguelen Islands (Southern Ocean) seen through weather regimes. *Journal of Applied Meteorology and Climatology*, 60, 711–731. <https://doi.org/10.1175/jamc-d-20-0255.1>.
- Poli, P., Hersbach, H., Dee, D.P., Berrisford, P., Simmons, A.J., Vitart, F., Laloyaux, P., Tan, D.G.H., Peubey, C., Thépaut, J.N., Trémolet, Y., Hólm, E.V., Bonavita, M., Isaksen, L. and Fisher, M. (2016) ERA-20C: an atmospheric reanalysis of the twentieth century. *Journal of Climate*, 29(11), 4083–4097. <https://doi.org/10.1175/JCLI-D-15-0556.1>.
- Prebble, J.G., Bostock, H.C., Cortese, G., Lorrey, A.M., Hayward, B. W., Calvo, E.C., Northcote, L.C., Scott, G.H. and Neil, H.L. (2017) Evidence for a Holocene climatic optimum in the Southwest Pacific: a multiproxy study. *Paleoceanography*, 32, 763–779. <https://doi.org/10.1002/2016PA003065>.
- Prince, H.D., Cullen, N.J., Gibson, P.B., Conway, J. and Kingston, D.G. (2021) A climatology of atmospheric rivers in New Zealand. *Journal of Climate*, 34(11), 4383–4402. <https://doi.org/10.1175/JCLI-D-20-0664.1>.
- Reid, K.J., Rosier, S.M., Harrington, L.J., King, A.D. and Lane, T.P. (2021) Extreme rainfall in New Zealand and its association with Atmospheric Rivers. *Environmental Research Letters*, 16(4), 044012. <https://doi.org/10.1088/1748-9326/abea0>.
- Renwick, J.A. (2011) Kidson’s synoptic weather types and surface climate variability over New Zealand. *Weather and Climate*, 31, 3–23. <https://doi.org/10.2307/26169715>.
- Renwick, J.A. and Thompson, D.W.J. (2006) The Southern Annular Mode and New Zealand climate. *Water and Atmosphere*, 14(2), 24–25.
- Salinger, M.J. (1979) New Zealand climate: the temperature record, historical data and some agricultural implications. *Climatic Change*, 2(2), 109–126. <https://doi.org/10.1007/BF00133218>.
- Salinger, M.J. (1980a) New Zealand climate: I. Precipitation patterns. *Monthly Weather Review*, 108, 1892–1904.
- Salinger, M.J. (1980b) New Zealand climate: II. Temperature patterns. *Monthly Weather Review*, 108, 1905–1912.
- Shu, J., Shamseldin, A.Y. and Weller, E. (2021) The impact of atmospheric rivers on rainfall in New Zealand. *Scientific Reports*, 11, 5869. <https://doi.org/10.1038/s41598-021-85297-0>.
- Slivinski, L.C., Compo, G.P., Sardeshmukh, P.D., Whitaker, J.S., McColl, C., Allan, R.J., Brohan, P., Yin, X., Smith, C.A., Spencer, L.J., Vose, R.S., Rohrer, M., Conroy, R.P., Schuster, D.C., Kennedy, J.J., Ashcroft, L., Brönnimann, S., Brunet, M., Camuffo, D., Cornes, R., Cram, T.A., Dominguez-Castro, F., Freeman, J.E., Gergis, J., Hawkins, E., Jones, P.D., Kubota, H., Lee, T.C., Lorrey, A.M., Luterbacher, J., Mock, C.J., Przybylak, R.K., Pudmenzky, C., Slonosky, V.C., Tinz, B., Trewin, B., Wang, X.L., Wilkinson, C., Wood, K. and Wyszyński, P. (2020) An evaluation of the performance of the twentieth century reanalysis version 3. *Journal of Climate*, 34(4), 1417–1438. <https://doi.org/10.1175/jcli-d-20-0505.1>.
- Straus, D.M., Corti, S. and Molteni, F. (2007) Circulation regimes: chaotic variability versus SST-forced predictability. *Journal of Climate*, 20(10), 2251–2272. <https://doi.org/10.1175/JCLI4070.1>.
- Sturman, A. and Quénol, H. (2013) Changes in atmospheric circulation and temperature trends in major vineyard regions of New Zealand. *International Journal of Climatology*, 33, 2609–2621. <https://doi.org/10.1002/joc.3608>.
- Sturman, A. and Wanner, H. (2001) A comparative review of the weather and climate of the Southern Alps of New Zealand and the European Alps. *Mountain Research and Development*, 21(4), 359–369. [https://doi.org/10.1659/0276-4741\(2001\)021\[0359:ACROTW\]2.0.CO;2](https://doi.org/10.1659/0276-4741(2001)021[0359:ACROTW]2.0.CO;2).
- Sturman, A.P., McGowan, H.A. and Spronken-Smith, R.A. (1999) Mesoscale and local climates in New Zealand. *Progress in Physical Geography*, 23(4), 611–635. <https://doi.org/10.1191/030913399677305474>.
- Sturman, A.P. and Tapper, N.J. (2006) *The Weather and Climate of Australia and New Zealand*, 2nd edition. Melbourne, VIC: Oxford University Press, 541 pp.
- Tait, A., Henderson, R., Turner, R. and Zheng, X. (2006) Thin plate smoothing spline interpolation of daily rainfall for New Zealand using a climatological rainfall surface.

- International Journal of Climatology*, 26(14), 2097–2115. <https://doi.org/10.1002/joc.1350>.
- Tait, A., Sturman, J. and Clark, M. (2012) An assessment of the accuracy of interpolated daily rainfall for New Zealand. *Journal of Hydrology (New Zealand)*, 51(1), 25–44.
- Tait, A. and Turner, R. (2005) Generating multiyear gridded daily rainfall over New Zealand. *Journal of Applied Meteorology*, 44(9), 1315–1323. <https://doi.org/10.1175/JAM2279.1>.
- Tao, L., Hu, Y. and Liu, J. (2016) Anthropogenic forcing on the Hadley circulation in CMIP5 simulations. *Climate Dynamics*, 46(9–10), 3337–3350. <https://doi.org/10.1007/s00382-015-2772-1>.
- Udy, D.G., Vance, T.R., Kiem, A.S., Holbrook, N.J. and Curran, M. A.J. (2021) Links between large-scale modes of climate variability and synoptic weather patterns in the southern Indian Ocean. *Journal of Climate*, 34(3), 883–899. <https://doi.org/10.1175/JCLI-D-20-0297.1>.
- Ummenhofer, C.C. and England, M.H. (2007) Interannual extremes in New Zealand precipitation linked to modes of Southern Hemisphere climate variability. *Journal of Climate*, 20(21), 5418–5440. <https://doi.org/10.1175/2007JCLI1430.1>.
- Ummenhofer, C.C., Sen Gupta, A. and England, M.H. (2009) Causes of late twentieth-century trends in New Zealand precipitation. *Journal of Climate*, 22(1), 3–19. <https://doi.org/10.1175/2008JCLI2323.1>.
- Wille, J.D., Favier, V., Gorodetskaya, I.V., Agosta, C., Kittel, C., Beeman, J.C., Jourdain, N.C., Lenaerts, J.T.M. and Codron, F. (2021) Antarctic atmospheric river climatology and precipitation impacts. *Journal of Geophysical Research: Atmospheres*, 126(8), e2020JD033788. <https://doi.org/10.1029/2020jd033788>.

## SUPPORTING INFORMATION

Additional supporting information can be found online in the Supporting Information section at the end of this article.

**How to cite this article:** Pohl, B., Sturman, A., Renwick, J., Quéno, H., Fauchereau, N., Lorrey, A., & Pergaud, J. (2022). Precipitation and temperature anomalies over Aotearoa New Zealand analysed by weather types and descriptors of atmospheric centres of action. *International Journal of Climatology*, 1–23. <https://doi.org/10.1002/joc.7762>